USGS
science for a changing world

Geologic Map of the Alamosa 30′ × 60′ Quadrangle, South-Central Colorado

Scientific Investigations Map 3342

U.S. Department of the Interior
U.S. Geological Survey

Geologic Map of the Alamosa 30′ × 60′ Quadrangle, South-Central Colorado

By Ren A. Thompson, Ralph R. Shroba, Michael N. Machette, Christopher J. Fridrich, Theodore R. Brandt, and Michael A. Cosca

Scientific Investigations Map 3342

U.S. Department of the Interior
U.S. Geological Survey

U.S. Department of the Interior
SALLY JEWELL, Secretary

U.S. Geological Survey
Suzette M. Kimball, Acting Director

U.S. Geological Survey, Reston, Virginia: 2015
Supersedes Open-File Report 2005–1392,
and Open-File Report 2008–1124

Suggested citation:
Thompson, R.A., Shroba, R.R., Machette, M.N., Fridrich, C.J., Brandt, T.R., and Cosca, M.A., 2015, Geologic map of the Alamosa 30′ × 60′ quadrangle, south-central Colorado: U.S. Geological Survey Scientific Investigations Map 3342, 23 p., scale 1:100,000, http://dx.doi.org/10.3133/sim3342. (Supersedes Open-File Report 2005–1392, and Open-File Report 2008–1124.)

ISSN 2329-132X (online)

Contents

Sheet

Figures

Tables

Conversion Factors

International System of Units to Inch/Pound

Multiply	By	To obtain
	Length	
centimeter (cm)	0.3937	inch (in.)
meter (m)	3.281	foot (ft)
kilometer (km)	0.6214	mile (mi)
	Area	
square kilometer (km^2)	0.3861	square mile (mi^2)

Temperature in degrees Celsius (°C) may be converted to degrees Fahrenheit (°F) as

$$°F = (1.8 \times °C) + 32$$

Temperature in degrees Fahrenheit (°F) may be converted to degrees Celsius (°C) as

$$°C = (°F - 32) / 1.8$$

Altitude, as used in this report, refers to distance above sea level.

Divisions of Quaternary, Neogene, and Paleogene Time Used in This Report[1]

Period or subperiod	Epoch		Age
Quaternary	Holocene		0–11.5 ka
	Pleistocene	late	11.5–132 ka
		middle	132–788 ka
		early	788 ka–2.588 Ma
Neogene	Pliocene		2.588–5.332 Ma
	Miocene		5.332–23.03 Ma
Paleogene	Oligocene		23.03–33.9 Ma
	Eocene		33.9–55.8 Ma
	Paleocene		55.8–65.5 Ma

[1]Ages of time boundaries are those of the U.S. Geological Survey Geologic Names Committee (2010) except those for the late-middle Pleistocene boundary and middle-early Pleistocene boundary, which are those of Richmond and Fullerton (1986). Ages are expressed in ka for kilo-annum (thousand years) and Ma for mega-annum (million years).

Geologic Map of the Alamosa 30′ × 60′ Quadrangle, South-central Colorado

By Ren A. Thompson, Ralph R. Shroba, Michael N. Machette, Christopher J. Fridrich, Theodore R. Brandt, and Michael A. Cosca

Introduction

The Alamosa 30′ × 60′ quadrangle is located in the central San Luis Basin of southern Colorado and is bisected by the Rio Grande having headwaters in the San Juan Mountains of Colorado and ultimately discharging into the Gulf of Mexico more than 3,000 kilometers (km) downstream. Alluvial floodplains and associated deposits of the Rio Grande and east-draining tributaries, La Jara Creek and Conejos River, occupy the north-central and northwestern part of the map area. Alluvial deposits of west-draining Rio Grande tributaries, Culebra and Costilla Creeks, bound the Costilla Plain in the south-central part of the map area. The San Luis Hills, a northeast-trending series of flat-topped mesas and hills, dominate the landscape in the central and southwestern part of the map and preserve fault-bound Neogene basin surfaces and deposits. The Precambrian-cored Sangre de Cristo Mountains rise to an elevation of nearly 4,300 meters (m), almost 2,000 m above the valley floor, in the eastern part of the map area. In total, the map area contains deposits that record surficial, tectonic, sedimentary, volcanic, magmatic, and metamorphic processes over the past 1.7 billion years (fig. 1; map sheet).

The mapped distribution of units is based primarily on interpretation of U.S. Geological Survey (USGS) 1:40,000-scale, black-and-white, aerial photographs; U.S. Department of Agriculture color orthoimagery (http://www.fsa.usda.gov/FSA/apfoapp?area=home&subject=prog&topic=nai); 2012 DigitalGlobe GeoEye satellite imagery (http://www.digitalglobe.com/resources/satellite-information); 1:24,000-scale USGS topographic maps and associated shaded-relief imagery; and, limited use of USGS lidar imagery (http://lidar.cr.usgs.gov/index.php). This geologic map compilation is based, in part, on previous mapping as indicated on the index (fig. 2; map sheet) to sources of geologic data, and reflects varying degrees of new synthesis and reinterpretation. Mapped surficial deposits and descriptions reflect reinterpretation and reclassification of units and revisions to geographic extent, and lithologic character and map unit representation particularly with respect to mapping of tills in glaciated valleys on the east flanks of the Sangre de Cristo Mountains and Culebra Range by Shroba.

Bedrock mapping represents a regional synthesis of geologic data compiled and published over the past quarter century and necessarily includes both simplification and expansion of previously published data with respect to the adopted stratigraphic nomenclature and aerial depiction of map units and faults. Regional and local unit nomenclature is constrained by reference to recently published and previously unpublished $^{40}Ar/^{39}Ar$ age determinations on Neogene volcanic deposits—the primary Cenozoic stratigraphic markers in the map area. Map unit descriptions rely heavily on previously published data and are simplified to embody the dominant characteristics of map units particularly where units depicted on larger-scale maps were combined for inclusion in this 1:100,000-scale map. Fault depictions are largely simplified and reflect our interpretation of the most regionally significant and better-exposed structures. Inferred faults that were previously mapped, particularly those buried beneath younger surficial deposits in the San Luis Valley, typically have large locational uncertainties and are poorly dated. Consequently, depiction of these buried faults on this map compilation is minimized (fig. 3; map sheet).

Surficial deposits were mapped and compiled by Machette and Shroba (2005–2013). Bedrock deposits were mapped and compiled by Thompson and Fridrich (2005–2013). All authors contributed to the fault compilation. Brandt prepared the digital topographic base map, digital compilation, and GIS database of the geologic map.

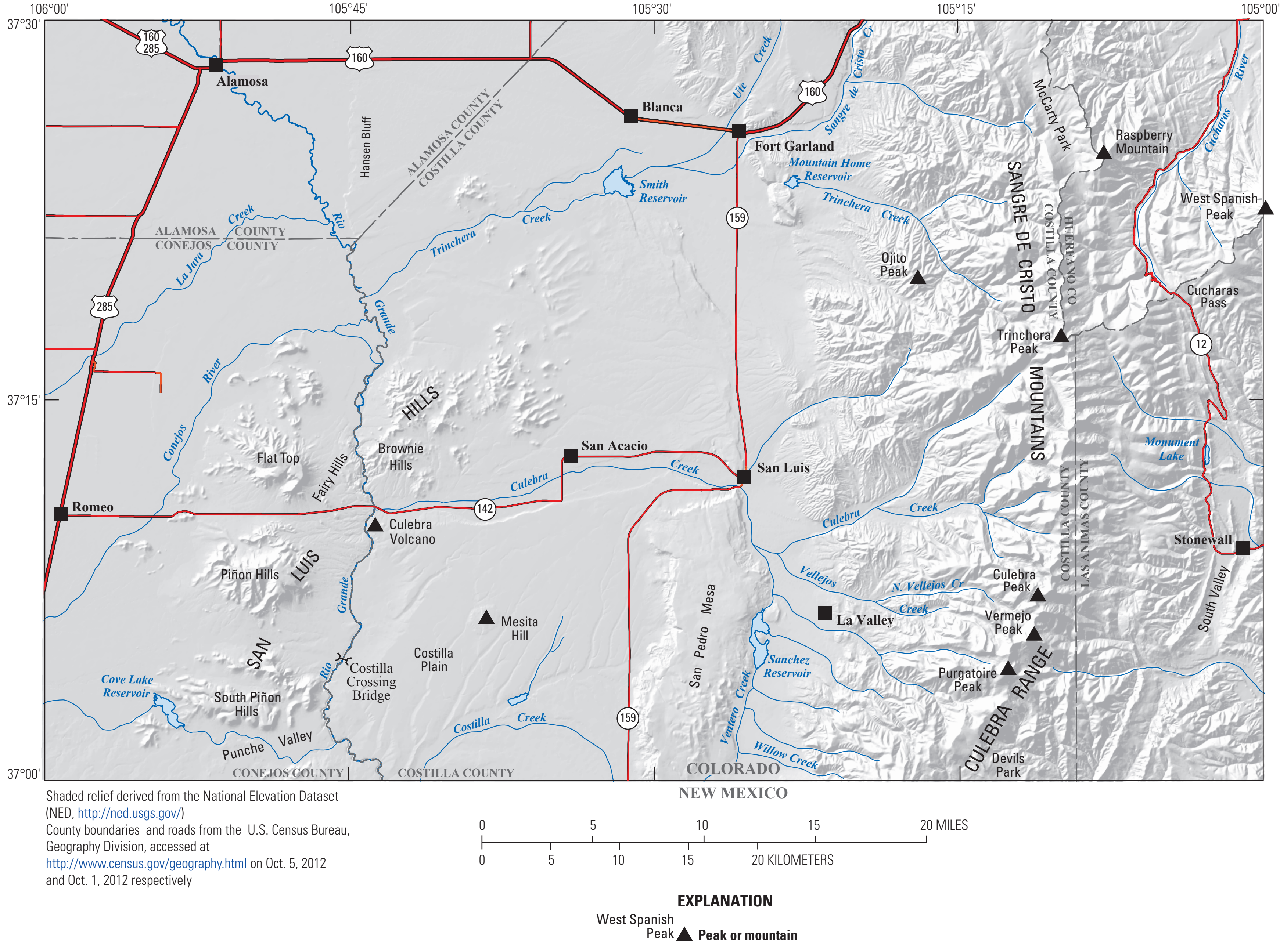

Figure 1. Shaded relief location index for Alamosa 30′ × 60′ quadrangle.

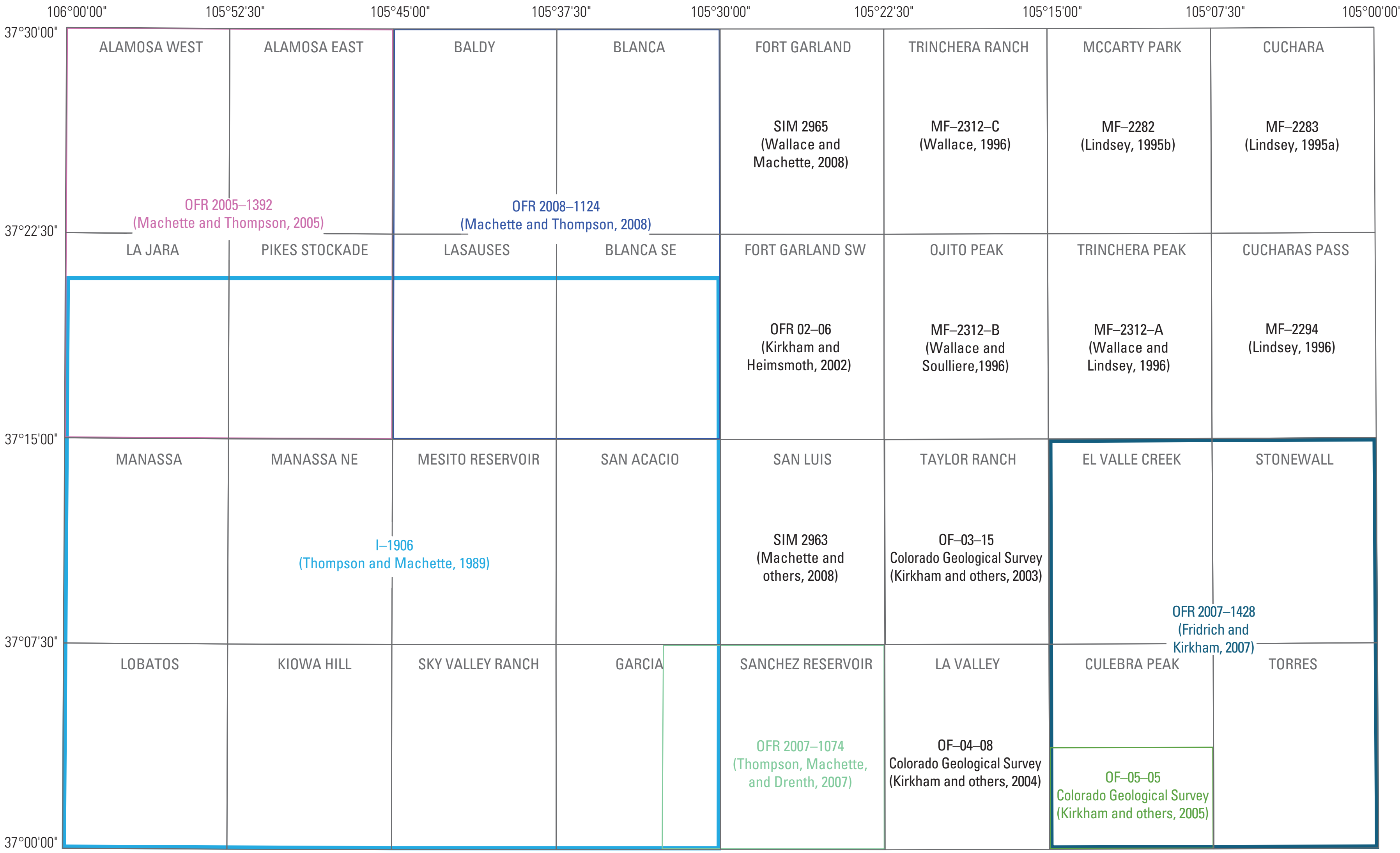

Figure 2. Index to geologic map data sources used in map compilation. For U.S. Geological Survey, publications the publication number, author(s), and year of publication are shown. For non-USGS publications, the State agency, author, and publication year are shown.

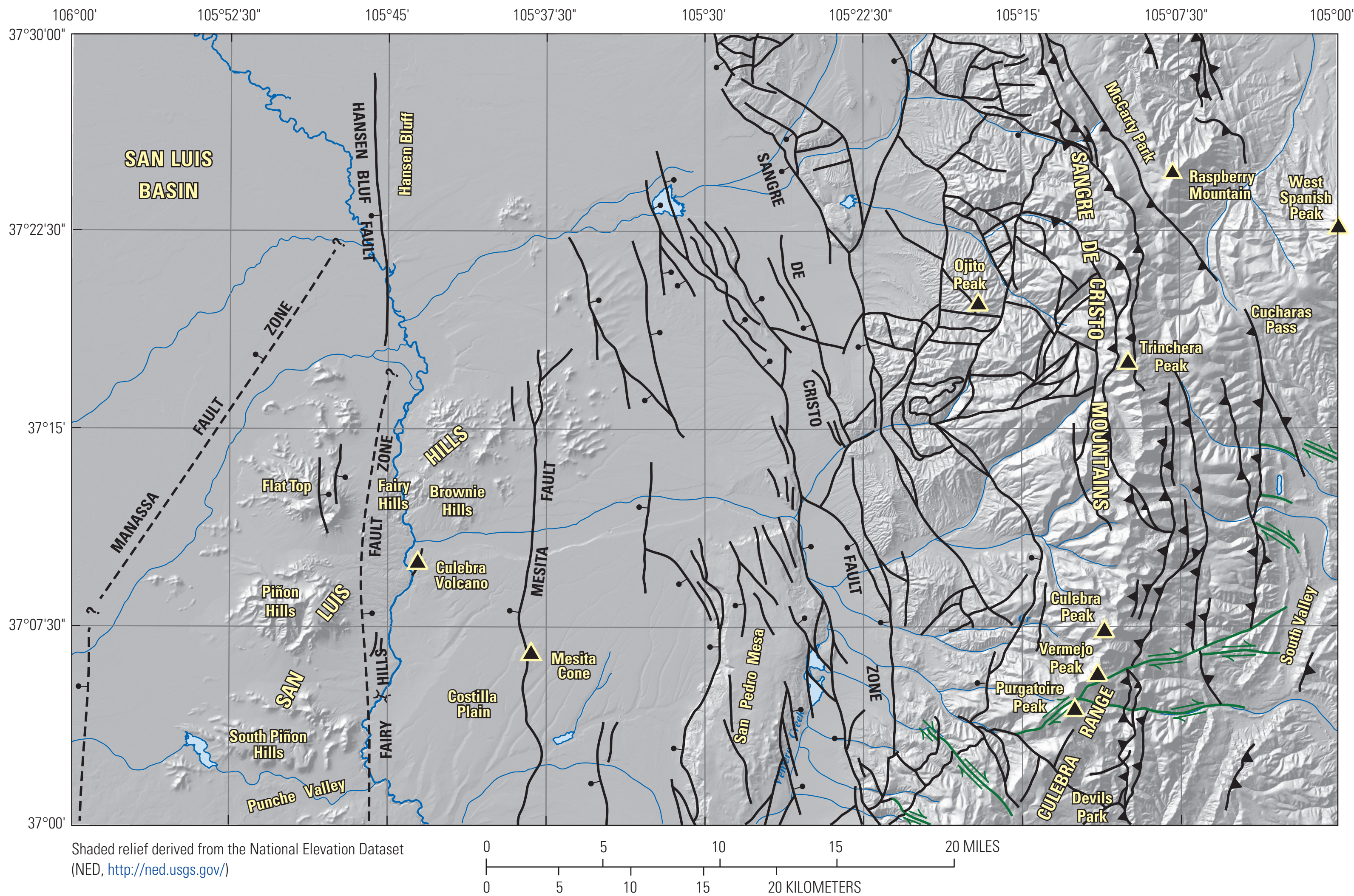

Figure 3. Simplified fault map for Alamosa 30′ × 60′ quadrangle showing major faults of the San Luis Basin and Sangre de Cristo Mountains. Older thrust-faults of the Sangre de Cristo Mountains are shown in black with thrust attribution. Post-thrust faults of indeterminate age are depicted in green with sense of oblique-slip displacement indicated by green arrows. Cenozoic extension-related faulting of the basin includes numerous dip-slip faults reflecting down-to-east or down-to-west displacement basinward of the numerous range-bounding faults of the Sangre de Cristo fault zone (solid black lines with bar and ball on downthrown side of fault). Dashed faults indicate faults or fault zones of Oligocene to Miocene age and are inferred based on geologic constraints exposed in adjacent bedrock or geophysical constraints. The location of the Manassa fault zone is derived from Drenth and others (2011). The Fairy Hills fault zone coincides with a zone of extensive hydrothermal alteration and mineralization exposed on the east side of South Piñon Hills, Piñon Hills and the Flat Top mesas west of the fault zone. The Fairy Hills are deeply incised remnants of altered Miocene and Oligocene volcanic deposits exposed along the Rio Grande near the Colo. Hwy 142 bridge crossing. The down-to-east sense of fault displacement is inferred from offset deposits of preserved Hinsdale lavas (Th) of Oligocene age on mesas west of the Rio Grande and in the Brownie Hills east of the Rio Grande, and is supported by geophysical modeling of Drenth and others (2013). Black triangles, mountain peak.

DESCRIPTION OF MAP UNITS

SURFICIAL DEPOSITS

The surficial units on this map are informal allostratigraphic units of the North American Stratigraphic Code (North American Commission on Stratigraphic Nomenclature, 1983) and are known or estimated to be at least 1 m thick. Many of these deposits are poorly exposed. Consequently, thickness determinations are often estimates or approximations. Age assignments for surficial deposits are based chiefly on: (1) the relative heights above modern streams or channels of ephemeral streams; (2) topographic relationships with other surficial deposits; and (3) to a lesser extent, relative degree of erosional modification of original (depositional) surface morphology. Soil-horizon designations are those of the Soil Survey Staff (1999) and Birkeland (1999). Stages of secondary calcium soil-carbonate morphology used in the descriptions are those of Machette (1985). Grain or particle sizes of surficial deposits are based on field estimates, using the modified Wentworth scale (American Geological Institute, 1982).

ARTIFICIAL-FILL DEPOSITS

af **Artificial fill (latest Holocene)—**Rock fragments and finer material in earth-fill dams that impound reservoirs, mine tailings, and mill-waste deposits produced at and near an open-pit mine about 5 km northeast of San Luis. Only deposits visible at map scale are shown. Thickness locally greater than 15 m

EOLIAN DEPOSITS

Qed **Eolian dune sand (Holocene)—**Wind-deposited sand that forms small, well-expressed dunes as much as 5 m high. Some dunes are active; others are inactive and have surface soils with weak A horizons. Unit locally includes small, inter-dune playa deposits that chiefly comprise organic silt and clay. Unit locally may include deposits of floodplain alluvium (Qfp), younger eolian sheet and dune sand (Qey), older eolian sheet and dune sand (Qeo), and younger alluvium (Qay). Radiocarbon ages of charcoal in buried soils in unit are 2,804±54, 3,905±98, and 5,560±90 cal. yr B.P., indicating at least three episodes of eolian deposition followed by episodes of surface stability (Machette and Puseman, 2007). Estimated thickness 1–5 m

Qey **Younger eolian sheet and dune sand (Holocene)—**Wind-deposited sand that forms thin sheets and small coppice (plant-stabilized) dunes. Multiple depositional units are common, often marked by organic-enriched buried soil A horizons formed in the tops of the units (Machette and Puseman, 2007). Unit locally may include deposits of eolian dune sand (Qed), older eolian sheet and dune sand (Qeo), and young stream alluvium (Qay). Linear deposits of unit, which locally overlie Servilleta Basalt (Tsb) on the south side of Smith Reservoir, locally include deposits of alluvium and colluvium, undivided (Qpo) and sheetwash alluvium. Thickness 1–3 m

Qeo **Older eolian sheet and dune sand (late Pleistocene)—**Wind-deposited sand forms thin sheets and small coppice (plant-stabilized) dunes east of the Rio Grande. Surface soils have weak Bt and Bk horizons, indicating surface stability after deposition. Unit locally may include deposits of eolian dune sand (Qed) and younger eolian sheet and dune sand (Qey). Thickness 1–3 m

SPRING/PALEOSPRING DEPOSITS

Qsm **Spring-mound deposit (Holocene)—**Porous tufa (calcium carbonate) forms spring mounds and channels and overlies the peat deposit (Qpt) in post-Pinedale stream valley graded to the Rio Grande, about 12 km west of Blanca. Radiocarbon ages of gastropod shells in the tufa range from 7 to 4 cal. yr B.P. (Schumann and Machette, 2007). Thickness <1 m

Qpt **Peat deposit (early Holocene and latest Pleistocene?)—**Wetland, organic-rich, silty and woody peat deposits in post-Pinedale stream valley graded to the Rio Grande, about 12 km west of Blanca, in the north-central part of the map area. Unit overlies deposits of younger alluvium (Qay), and is locally overlain by spring-mound deposit (Qsm). Radiocarbon ages of organic carbon from unit range from 13.5 to 7 cal. yr B.P. (Schumann and Machette, 2007). Thickness unknown; possibly 1–5 m

LACUSTRINE DEPOSITS

Qlp **Lake and pond deposits (Holocene and latest Pleistocene?)—**Mostly ponded sediments that accumulated in and near small, ephemeral, natural lakes and ponds, and man-made lakes. Typically, deposits are fine grained (silty and clayey), but locally may be sandy or pebbly at or near margins of water bodies. Unit locally may include deposits of sheetwash alluvium as well as organic-rich marsh and bog deposits in wetland environments in glaciated areas in and near the Sangre de Cristo Mountains and Culebra Range. Thickness unknown; possibly 1–5 m

Qlal **Lagoonal deposits of Lake Alamosa (middle Pleistocene)—**Fine-grained deposits, composed chiefly of sand and silt, that accumulated in lagoons and ponds impounded by barrier bars and spits of unit Qlas formed along the shore of ancient Lake Alamosa chiefly by wave action and longshore drift. Exposed thickness commonly 2–5 m

Qlas **Shoreline deposits of Lake Alamosa (middle Pleistocene)—**Locally derived coarse sand and gravel deposited in barrier bars and spits along the shorelines of ancient Lake Alamosa. Mainly preserved at elevations of 2,330–2,340 m (7,645–7,676 ft) on northern margin of the San Luis Hills. Strongly developed calcic soils (with Bk and K horizons) and ^{3}He/^{4}He surface-exposure dating of relict beach boulders on unit suggest that the lake overflowed through the San Luis Hills at about 430 ka (Machette and others, 2007, 2013). Exposed thickness commonly 2–20 m

QTla **Alamosa Formation of Siebenthal (1910) (middle Pleistocene to Pliocene)—**Closed-basin lacustrine deposits related to alternating, climatically driven shallow- and deep-water phases of ancient Lake Alamosa. Unit is characterized by thick clay (and probably silty clay) beds and thin sand beds in the deeper parts of the lake basin near the town of Alamosa and along the eastern margin of the basin, and by clay, silt, and sand beds in shallower parts of the basin, which are interstratified with deposits of fluvial sand and gravel near former shorelines. Unit contains a bed of Bishop ash at Hansen Bluff (Rogers and others, 1985, 1992), about 13 km southeast of Alamosa, which has a ^{40}Ar/^{39}Ar mean age of 759±2 ka (Sarna-Wojcicki and others, 2000). Strongly developed calcic soils and ^{3}He surface-exposure dating suggest that the lake overflowed through the San Luis Hills at about 430 ka (Machette and others, 2007, 2013). Maximum thickness about 400 m (Siebenthal, 1910) or possibly greater than 550 m near the eastern margin of the San Luis Valley (Huntley, 1979); much thinner along and near former shorelines

ALLUVIAL DEPOSITS

Qaa **Channel alluvium (late Holocene)—**Consists chiefly of coarse sand and pebble to small-cobble gravel in modern and recently active stream channels that are incised into older alluvial deposits. Top of unit has well-preserved depositional morphology and commonly is at or just above modern stream level. Unit locally includes minor deposits of floodplain alluvium (Qfp); locally may include small deposits of younger alluvium (Qay) and young alluvium, undivided (Qau). Thickness unknown; possibly 1–5 m

Qa **Channel and floodplain alluvium, undivided (Holocene)—**Silty clay, silt, sand, and pebble to small-cobble gravel. Unit is composed of deposits of channel alluvium (Qaa) and floodplain alluvium (Qfp) that are too small to show separately at map scale. Unit Qa locally includes unmapped deposits of sheetwash alluvium and small deposits of younger alluvium (Qay). Terrace surfaces 1–10 m above modern streams (table 1). Thickness unknown; possibly 1–5 m

Qau **Young alluvium, undivided (Holocene and late Pleistocene)—**Silty clay and silt to cobbly pebble gravel. Unit is composed chiefly of deposits of units Qa and Qay, and locally includes unmapped deposits of unit Qac along and near valley sides, and deposits of sheetwash alluvium. Deposits locally consist of fill or partly fill stream channels and locally underlie floodplains and low terraces that are <1–10 m above modern streams (table 1). Unit is locally mapped along the mountainous reaches of westward-flowing streams in the Sangre de Cristo Mountains and Culebra Range as well as in the adjacent alluvial piedmont on the east side of San Pedro Mesa near La Valley and San Luis (fig. 1). Unit Qau locally includes unmapped deposits of glacial outwash deposited in glaciated valleys during the Pinedale glaciation. Thickness unknown; possibly 1–10 m

Table 1. Approximate height, in meters, of the top of selected alluvial units above modern stream level in the Alamosa 30′ × 60′ quadrangle. Unit heights vary depending on proximity to major stream and active Quaternary faults.

[Unit Qau is composed chiefly of deposits of units Qa and Qay, and locally includes unmapped deposits of unit Qac along and near valley sides and deposits of sheetwash alluvium. Unit Qau is not listed separately; —, no deposits]

Map unit	Rio Grande	Major tributaries to the Rio Grande in the western half of the quadrangle	Major streams in the piedmont on the west side of the Culebra Range east of San Pedro Mesa	Mountainous reaches of major streams west of the crests of the Sangre de Cristo Mountains and Culebra Range	Major streams near the eastern boundary of the quadrangle
Qa	—	—	1–2	1–10	—
Qay	5–10	1–2	2	5–10	5
Qai	18–22	2–5	5	25–35	25–60
Qao	50–60	5–15	25	60–120	65–80

Qfp **Floodplain alluvium (Holocene)—**Commonly consists of silty clay, silt, very fine- to medium-grained sand, and lenses of pebble gravel. The top of unit has muted depositional morphology and commonly is <1 m above the top of inset deposits of channel alluvium (Qaa). Unit commonly has very weakly developed surface soils with weakly oxidized C (Cox) horizons. Unit locally includes deposits of unit Qaa that are too small to show at map scale, and locally may include deposits of unit Qay. Thickness unknown; possibly 1–5 m

Qay **Younger alluvium (late Pleistocene)—**Fluvial sand, pebble gravel, and cobbly pebble gravel beneath terrace surfaces, at one and locally at two levels, that are 1–2 to 5–10 m above modern streams (table 1) depending on proximity to major stream and active Quaternary faults. Unit commonly has weakly developed surface soils with Bw (cambic), weak Bt (argillic), and (or) Bk (carbonate-enriched) horizons. Bk horizons have stage I to weak stage II carbonate morphology. Soil morphology suggests that unit was deposited during the Pinedale glaciation (Thompson and Machette, 1989). Unit locally includes deposits of glacial outwash deposited in glaciated valleys during the Pinedale glaciation, deposits of units Qaa and Qfp along and near minor streams, and deposits of unit Qac along and near valley sides; these included deposits that are too small to show at map scale. Unit also locally includes unmapped deposits of sheetwash alluvium, and may include deposits of young alluvium, undivided (Qau). Thickness 5–10 m along the Rio Grande; unknown elsewhere

Qai **Intermediate alluvium (late and middle Pleistocene)—**Fluvial sand and gravel beneath terrace surfaces, at one and locally at two levels, that are 2–5 and 25–60 m above modern streams (table 1) depending on proximity to major stream and active Quaternary faults. Unit commonly has moderately developed surface soils with Bt and Bk horizons. Bk horizons have stage II to III carbonate morphology. Soil morphology suggests that unit Qai was deposited during the Bull Lake glaciation (Thompson and Machette, 1989). Unit locally includes unmapped deposits of glacial outwash deposited in glaciated valleys during the Bull Lake glaciation and unmapped deposits of unit Qac along and near valley sides, and deposits of sheetwash alluvium. Unit locally may include deposits of unit Qao. Thickness 5–10 m along the Rio Grande; unknown elsewhere

Qao **Older alluvium (middle Pleistocene)—**Fluvial sand and gravel beneath alluvial surfaces that are 5–120 m above modern streams (table 1) depending on proximity to major stream and active Quaternary faults. Unit commonly has strongly developed surface soils with thick, clayey, reddish-brown Bt horizons above Bk and K horizons with stage III to IV carbonate morphology, respectively. Unit predates or mostly predates shoreline deposits of Lake Alamosa (Qlas). About 3 km northeast of San Luis, unit locally overlies a bed of Lava Creek B ash near the eroded top of unit QTsf (Machette and others, 2008). Lava Creek B ash has a $^{40}Ar/^{39}Ar$ mean age of 639±2 ka (Lanphere and others, 2002). Unit may have been deposited during one or more pre-Bull Lake glaciations that occurred after 640 ka. Unit locally includes unmapped deposits of unit Qac and deposits of sheetwash alluvium, and locally may include deposits of unit Qai as well as glacial outwash of pre-Bull Lake age. Thickness at least 10 m along the Rio Grande and Culebra Creek; unknown elsewhere

ALLUVIAL AND COLLUVIAL DEPOSITS

Qpy **Younger piedmont-slope deposits (late Pleistocene)—**Chiefly fine- to coarse-grained alluvium and debris-flow deposits that underlie broad, mostly undissected piedmont surfaces adjacent to the San Luis Hills. Sediment commonly ranges in size from silty sand to pebbly and cobbly gravel. Commonly has weakly developed surface soils with Bk horizons that have stage I to II carbonate morphology. Unit Qpy locally includes unmapped deposits of sheetwash alluvium and colluvium (Qc). Thickness unknown; possibly 1–15 m

Qac **Alluvium and colluvium, undivided (Holocene to middle? Pleistocene)—**Chiefly undifferentiated silty, sandy, and gravelly stream alluvium, sandy sheetwash alluvium, stony debris-flow (fan) deposits, colluvium (Qc), and locally other mass-movement deposits along minor streams and on adjacent lower (toe) slopes in and near the Sangre de Cristo Mountains and Culebra Range. Unit locally includes deposits of outwash deposited in glaciated valleys during the Pinedale glaciation (Qtp); locally may include deposits of unit Qay and Qau. Thickness unknown; possibly 3–50 m

Qpo **Older piedmont-slope deposits (late and middle Pleistocene)—**Chiefly fine- to coarse-grained alluvium and debris-flow deposits that underlie dissected piedmont surfaces at multiple levels near the San Luis Hills and the South Fork Purgatoire River, near the southeastern corner of the map area (fig. 1). Sediment commonly ranges in size from silty sand to pebbly and cobbly gravel. Unit commonly has moderately to strongly developed surface soils with reddish-brown Bt horizons above Bk horizons, with stage II to III carbonate morphology. Unit locally includes unmapped deposits of sheetwash alluvium and colluvium (Qc). Thickness unknown; possibly 1–15 m

MASS-MOVEMENT DEPOSITS

Colluvial Deposits

Qc **Colluvium (Holocene to middle? Pleistocene)—**Deposits composed of non-sorted to very poorly sorted and non-stratified to crudely stratified, mostly matrix-supported, sandy sediment and rock debris typically on moderate to steep slopes formed on the Santa Fe Group and older bedrock units. Unit includes diamicton deposits mapped by Kirkham and others (2004) in Devils Park in southeast part of map area. Unit locally includes landslide deposits, undivided (Qls) that have muted surface morphology, as well as talus deposits (Qta) and rock-glacier deposits (Qrg) near the heads of glaciated valleys. Unit locally may include unmapped deposits of sheetwash alluvium. Thickness unknown; possibly 1–50 m

Qta **Talus deposits (Holocene to middle? Pleistocene)—**Very poorly sorted, crudely stratified, very angular and angular boulders and smaller rock fragments deposited chiefly by rock and snow avalanche, rock fall, rock slide, and debris flow at the base of cliffs and steep slopes where debris locally forms broad aprons, small cones, and fan-shaped deposits. Unit locally includes rubbly scree deposits and small debris-flow deposits. Commonly derived from Servilleta Basalt (Tsb) and Paleoproterozoic crystalline bedrock. Unit includes two large rockfall deposits, which likely formed on snow or ice, near the headwaters of North Vallejos Creek on the northwest side of Vermejo Peak and near the headwaters of Bernardino Creek on the west side of Miranda Peak. Unit locally includes small deposits of colluvium (Qc) and rock-glacier deposits (Qrg). Thickness unknown; possibly 1–15 m

Landslide Deposits

Qls **Landslide deposits, undivided (Holocene to middle Pleistocene)—**Deposits composed of unsorted and unstratified debris of various sizes commonly at or near the base of moderate to steep slopes downslope of resistant bedrock units, such as Servilleta Basalt (unit Tsb). Unit locally includes small deposits of colluvium (Qc). Thickness unknown; possibly 5–50 m

Qlsy **Younger landslide deposits (Holocene and late Pleistocene)—**Commonly composed of large blocks and slabs of Servilleta Basalt (Tsb) in a matrix derived from sediment of the lower part of Santa Fe Group (Tsf) on moderate to steep slopes downslope of bedrock cliffs.

Younger landslide deposits commonly have a hummocky surface, sediment-filled closed depressions, and lobate toes. Some surface features suggest flowage, perhaps during former moist climatic episodes during the late Pleistocene. Commonly mapped in areas adjacent to basalt-covered hills and San Pedro Mesa. Unit locally includes small deposits of older landslide deposits (Qlso), landslide blocks (Qlsb), and colluvium (Qc). Thickness unknown; possibly 5–50 m

Qlso **Older landslide deposits (late and middle Pleistocene)—**Commonly composed of large blocks and slabs of Servilleta Basalt (Tsb) in a matrix derived from sediment of the lower part of Santa Fe Group (Tsf) on moderate to steep slopes downslope of bedrock cliffs. Older landslide deposits commonly also have subdued surface morphology owing to erosion and, locally, thick mantles composed of eolian sand, sheetwash alluvium and (or) colluvium (Qc). Unit locally includes small deposits of younger landslide deposits (Qlsy) and landslide blocks (Qlsb). Some older landslide deposits have abrupt, linear toes resulting from displacement by faults of the Sangre de Cristo fault system (Thompson and others, 2007; Machette and others, 2008). Mapped in areas adjacent to basalt-covered hills and San Pedro Mesa. Thickness unknown; possibly 5–50 m

Qlsb **Landslide blocks (Holocene to middle Pleistocene)—**Extremely large slabs of relatively coherent Servilleta Basalt (Tsb) displaced downslope by sliding on sediments of the lower part of Santa Fe Group (Tsf) on moderate to steep slopes. Unit locally includes small deposits of younger landslide deposits (Qlsy), older landslide deposits (Qlso), and colluvium (Qc). Deposits are common on moderate to steep slopes along the margins of basalt-covered hills and San Pedro Mesa, all of which have been uplifted by faults of the Sangre de Cristo fault system. Unit locally includes stratigraphically in-place, but structurally rotated bodies of Servilleta Basalt (Tsb). Thickness unknown; possibly locally as much as 50 m

GLACIAL DEPOSITS

Qrg **Rock-glacier deposits (Holocene? and latest Pleistocene?)—**Lobate and tongue-shaped masses of boulder- to silt-sized rock debris that commonly have steep fronts and flanks and form along valley walls and on valley floors above an elevation of about 3,250 m in the Sangre de Cristo Mountains, commonly in areas of high talus production. Deposits consist of a veneer of angular boulders that overlies a thick mass of smaller debris. Rock material accumulated chiefly as talus deposits that are mobilized downslope, possibly by flowage owing to the deformation of interstitial ice or an ice core. Lobate rock glaciers formed along valley walls, and are ice-cemented. Tongue-shaped rock glaciers resemble glaciers, form on valley floors, and commonly have debris-covered ice cores (Benedict, 1973; White, 1976). Ice-cemented rock glaciers likely formed under periglacial conditions (Barsch, 1987), whereas ice-cored rock glaciers probably are debris-covered glaciers (Janke, 2007). Rock fragments on and within rock-glacier deposits are derived from steep slopes chiefly by rockfall and locally by sliding and avalanche. Unit locally may include minor talus deposits (Qta) displaced by post-depositional creep or flowage, colluvium (Qc), other mass-movement deposits, and possibly till of Pinedale age (Qtp). Many of the rock-glacier deposits in Colorado are of latest Pleistocene or early Holocene age (Meierding and Birkeland, 1980). Thickness unknown; possibly locally as much as 50 m

Till (late and middle Pleistocene)—Mostly non-sorted and non-stratified, subangular to subrounded boulders to granules in a sand, silty sand, or slightly clayey, silty sand matrix deposited by glaciers in glaciated valleys above an elevation of about 2,750 m. Terminal moraines near the down-valley limit of glaciation may be composed, in part, of outwash sand and gravel. Deposits on the western flanks of the Sangre de Cristo Mountains and Culebra Range are rich in clasts composed chiefly of gneiss derived from Paleoproterozoic crystalline bedrock, whereas deposits on the eastern flank commonly are rich in clasts of terrestrial sedimentary rocks derived from the Sangre de Cristo Formation (P*P*s), and also locally contain clasts of marine and non-marine sedimentary rocks of the Madera Formation (*P*m)

Qti **Till of Pinedale age and till of Bull Lake age, undivided (late and middle Pleistocene)—** Unit is mapped in glaciated valleys on the east flanks of the Sangre de Cristo Mountains and Culebra Range where till of Pinedale age (Qtp) cannot be distinguished from till of Bull Lake age (Qtb) and (or), possibly, till of pre-Bull Lake age. Unit consists chiefly of Pinedale age till (Qtp). See descriptions for units Qtp and Qtb

Qtp **Till of Pinedale age (late Pleistocene)—**Unit commonly forms large prominent, sharp-crested lateral and terminal moraines that are very bouldery and have distinct constructional morphology. Deposits locally have unfilled and undrained kettles, moraine-dammed lakes, and swamps. Surface soils formed in till of Pinedale age, which is derived chiefly from Paleoproterozoic crystalline bedrock, probably have thin Bw or thin, weakly developed Bt horizons. Deposits derived chiefly from Paleozoic sedimentary bedrock, have thin weakly or moderately developed Bt horizons. Unit probably locally includes deposits of stratified drift deposited by glacial meltwater, till of Bull Lake age (Qtb), colluvium (Qc), other mass-movement deposits, young alluvium, undivided (Qau), and younger alluvium (Qay); locally may include small areas of bedrock near the down-valley limit of glaciation. Radiocarbon and cosmogenic-exposure ages indicate that till of Pinedale age is about 12–30 ka (Nelson and others, 1979; Madole, 1986; Schildgen and Dethier, 2000; Benson and others, 2004, 2005, 2007), although some deposits may be correlative with an early advance of Pinedale ice in the northern Yellowstone area at about 34–47 ka (Sturchio and others, 1994) or with an earliest Pinedale advance at about 50–70 ka at McCall, Idaho, and in the Wind River Range near Lander, Wyo. (Dahms, 2004; Pierce and others, 2011). Thickness unknown; possibly 2–30 m

Qtb **Till of Bull Lake age (late and middle Pleistocene)—**Unit commonly forms prominent lateral moraines that have rounded crests beyond the outer limit of till of Pinedale age (Qtp). Undrained depressions are uncommon. Surface soils formed in till of Bull Lake age derived chiefly from Paleoproterozoic crystalline bedrock, probably have moderately developed Bt horizons. Soils formed in till of Bull Lake age derived chiefly from Paleozoic sedimentary bedrock, probably have moderately developed or well-developed Bt horizons. Unit probably locally includes stratified drift deposited by glacial meltwater, till of Pinedale age (Qtp), colluvium (Qc), and other mass-movement deposits; locally may include till of pre-Bull Lake age and small areas of bedrock near the down-valley limit of glaciation. K-Ar and ^{230}Th/U analyses for correlative deposits in Wyoming suggest that till of Bull Lake age is about 120–170 ka (Sharp and others, 2003; Pierce, 2004). ^{10}Be ages for the West Yellowstone glacial system yield a mean age of 136±13 ka and oldest ages of about 151–157 ka (Licciardi and Pierce, 2008). Thickness unknown; possibly 2–30 m

BASIN-FILL SEDIMENTARY DEPOSITS

QTsf **Santa Fe Group, upper part (middle Pleistocene to Pliocene)—**Unit is mapped as an informal upper member of the Santa Fe Group where it lies on or above Servilleta Basalt (Tsb). Sediments commonly are composed of poorly consolidated sandstone, siltstone, and pebble-to-cobble conglomerate. Generally, these sediments are less deformed, less oxidized, and include fewer playa-like (basin-center) deposits than those in lower part of Santa Fe Group (Tsf). Unit QTsf locally includes a bed of Lava Creek B ash near San Luis (Machette and others, 2008), which has a ^{40}Ar/^{39}Ar mean age of 639±2 ka (Lanphere and others, 2002). Thickness about 100–200 m, at and west of San Pedro Mesa; about 350 m thick in Energy Operating Co. Williamson No. 1 drill hole (Kirkham and others, 2004) on the east side of San Pedro Mesa

Tsf **Santa Fe Group, lower part (Pliocene to Oligocene)—**Unit is mapped as an informal lower member of the Santa Fe Group where it underlies Servilleta Basalt (Tsb) north and east of the central Sangre de Cristo fault system where it composes the majority of Santa Fe Group. Sediments of unit Tsf commonly are composed of moderately consolidated sandstone, siltstone, and pebble-to-cobble conglomerate. Generally, these sediments are more deformed, more oxidized, and include more playa-like (basin-center) deposits than those in upper part of Santa Fe Group (QTsf). Thickness unknown owing to poor exposure and faulting; about 1,500 m thick in Energy Operating Co. Williamson No. 1 drill hole (Kirkham and others, 2004) on the east side of San Pedro Mesa

Tsfv **Santa Fe Group, volcaniclastic deposits (Miocene and Oligocene)—**This informal member of the Santa Fe Group is similar in lithology to that of unit Tsf, except that unit Tsfv contains more beds and lenses of conglomerate as well as abundant (≥50 percent) clasts of Tertiary volcanic rocks. Deposits of unit Tsfv are light gray owing to abundant volcanic clasts and have a matrix rich in volcanic detritus. In addition to volcanic clasts, unit Tsfv also contains clasts composed of Paleozoic limestone and arkose and a subordinate amount of Paleoproterozoic gneiss. Unit Tsfv is locally exposed in the Culebra Range near Fort Garland and in rounded hills on northeast side of the San Luis Hills, southwest of Smith Reservoir, and in the Sangre de Cristo Mountains. Thickness >1,100 m near Fort Garland; possibly >2,000 m in the Ojito Peak 7.5-minute quadrangle southeast of Fort Garland

VOLCANIC ROCKS

Qba **Basaltic andesite of Mesita cone (early Pleistocene)—**Dark gray to black, xenocrystic basaltic andesite that forms a small shield volcano consisting of thin a′a lava flows and an overlying cone composed primarily of reddish brown to black cinder and spatter agglutinate. Most of the cone has been removed by open-pit cinder mining (Thompson, Machette, Shroba, and others, 2007). $^{40}Ar/^{39}Ar$ analysis of groundmass concentrate yielded an apparent age of 1.03±0.01 Ma (Appelt, 1998) and a whole-rock $^{40}Ar/^{39}Ar$ age determination of 1.06±0.04 Ma was obtained from a lava flow in the vent area of Mesita cone (sample RGR-03; table 2). Thickness approximately 15 m, base not exposed

Tsb **Servilleta Basalt (Pliocene)—**Vesicular to massive, thin flows of dark-gray to black tholeiitic basalt characterized by small olivine phenocrysts; flows locally have columnar joints and pahoehoe surface texture. Basalt is composed of millimeter-size plagioclase and olivine phenocrysts in a microcrystalline groundmass typically characterized by diktytaxitic texture (that is, jagged, irregular vesicles bounded by crystals). The uppermost lava flow at the Costilla Crossing Bridge yielded an $^{40}Ar/^{39}Ar$ apparent age of 4.21±0.13 Ma (sample RGR–02; table 2). A lava flow capping the west side of San Pedro Mesa yielded an apparent age of 3.79±0.05 Ma (sample SR12; table 2), whereas a lava flow at the northwest corner of the mesa yielded an apparent age of 4.74±0.19 (sample SA–MM06–90; table 2). Approximately 2 km north of the town of San Luis in Colorado, lava flows of the east margin of San Pedro mesa yielded ages of 4.59±0.08 Ma and 4.49±0.08 Ma (samples DM–99–53, DM–99–53c; table 2) and 4.59±0.02 Ma (sample DM–99–53a; table 2) at the north end of the mesa. A younger age of 3.66±0.12 Ma was obtained from a lava flow capping the low mesa along the Sangre de Cristo fault zone 4 km southeast of Fort Garland (sample DM–99–55; table 2). Appelt (1998) and Miggins (2002) report $^{40}Ar/^{39}Ar$ groundmass concentrate ages ranging from 3.66 Ma to 4.7 Ma in the map area. Surface exposures are more extensive to the south on the Taos Plateau of northern New Mexico where exposures in the Rio Grande gorge 16 km northwest of Taos, New Mexico, reach a maximum exposed thicknesses of approximately 175 m. Here, Cosca and others (2014) report $^{40}Ar/^{39}Ar$ apparent ages of 4.78±0.03 Ma at river level and 3.59±0.08 Ma at the top of the section. At the confluence of the Red River and the Rio Grande, 38 km south of the state line, Thompson and others (2013) report $^{40}Ar/^{39}Ar$ age determinations as old as 5.2 Ma for lavas at the base of the exposed Servilleta Basalt section. Near the border with New Mexico in the southern part of the map area, thicknesses in the gorge are approximately 40 m; base not exposed

Toa **Olivine andesite (Pliocene)—**Vesicular to massive, thin flows of dark-gray to black, sparsely to moderately porphyritic andesite containing olivine phenocrysts and moderately to highly flattened vesicles. Preserved as flow remnants beneath Servilleta shield volcano 4 km west of the Rio Grande in the southern part of the map area and forms an isolated shield volcano (Volcano de la Culebra of Burroughs, 1972) at the confluence of the Rio Grande and Culebra Creek. $^{40}Ar/^{39}Ar$ analysis of groundmass concentrate yielded an apparent age of 5.19±0.11 Ma (sample SLH501; table 2) from a lava flow exposed along the Rio Grande. Thickness 10–45 m, base not exposed

Table 2. Age determinations for select samples in the map area.

Sample no.	Location (UTM-NAD83)		Age (Ma)	Age type—Material analysed	Lab/analyst[1]
	Easting	Northing	± 2 sigma error		
ACX–99	475847	4101500	1,688±7	U-Pb age—zircon	USGS/W. Premo
BL–MM06–92	452059	4137915	3.79±0.17	$^{40}Ar/^{39}Ar$—groundmass concentrate, plateau age	USGS/D. Miggins
CF 7–28–09–1	477696	4104732	1,716±6	U-Pb age—zircon	USGS/W. Premo
CF 7–28–09–3	480450	4104225	1,714±18	U-Pb age—zircon	USGS/W. Premo
CF 7–28–09–4	480351	4103512	1,703±5	U-Pb age—zircon	USGS/W. Premo
DM–98–14	479347	4099121	12.08±0.06	$^{40}Ar/^{39}Ar$—hornblende, plateau age	USGS/D. Miggins
DM–98–16	478260	4098970	11.98±0.03	$^{40}Ar/^{39}Ar$—hornblende, plateau age	USGS/D. Miggins
DM–98–22–2	479740	4098134	11.87±0.03	$^{40}Ar/^{39}Ar$—hornblende, plateau age	USGS/D. Miggins
DM–98–22–7	479740	4098134	11.90±0.21	$^{40}Ar/^{39}Ar$—hornblende, plateau age	USGS/D. Miggins
DM–98–33–3	490677	4135515	23.59±0.15	$^{40}Ar/^{39}Ar$—hornblende, plateau age	USGS/D. Miggins
DM–98–43	494512	4131269	21.18±0.11	$^{40}Ar/^{39}Ar$—hornblende, plateau age	USGS/D. Miggins
DM–98–44	496009	4123441	22.90±0.16	$^{40}Ar/^{39}Ar$—hornblende, plateau age	USGS/D. Miggins
DM–98–45	496124	4104767	21.92±0.03	$^{40}Ar/^{39}Ar$—hornblende, plateau age	USGS/D. Miggins
DM–98–47	496205	4123009	21.98±0.16	$^{40}Ar/^{39}Ar$—hornblende, plateau age	USGS/D. Miggins
DM–99–51	466369	4098304	4.37±0.17	$^{40}Ar/^{39}Ar$—groundmass concentrate, plateau age	USGS/D. Miggins
DM–99–53	461654	4119515	4.59±0.08	$^{40}Ar/^{39}Ar$—groundmass concentrate, plateau age	USGS/D. Miggins
DM–99–53a	461235	4123928	4.59±0.02	$^{40}Ar/^{39}Ar$—groundmass concentrate, plateau age	USGS/D. Miggins
DM–99–53c	461730	4119548	4.49±0.08	$^{40}Ar/^{39}Ar$—groundmass concentrate, plateau age	USGS/D. Miggins
DM–99–54	464325	4125195	4.55±0.10	$^{40}Ar/^{39}Ar$—groundmass concentrate, plateau age	USGS/D. Miggins
DM–99–55	463717	4139427	3.66±0.12	$^{40}Ar/^{39}Ar$—groundmass concentrate, plateau age	USGS/D. Miggins
DM–99–59	495714	4124396	22.24±0.23	$^{40}Ar/^{39}Ar$—hornblende, plateau age	USGS/D. Miggins
DM–99–68	499210	4101068	22.65±0.10	$^{40}Ar/^{39}Ar$—hornblende, plateau age	USGS/D. Miggins
DM–99–71	490807	4096544	25.85±0.55	$^{40}Ar/^{39}Ar$—hornblende, plateau age	USGS/D. Miggins
DM–99–73	497039	4108618	22.19±0.21	$^{40}Ar/^{39}Ar$—hornblende, plateau age	USGS/D. Miggins
DM–99–79	497324	4147258	21.86±0.79	$^{40}Ar/^{39}Ar$—hornblende, plateau age	USGS/D. Miggins
EVC–CF05–8	483062	4119768	1691±5	U-Pb age—zircon	USGS/W. Premo
JI–1XGG1	473237	4096115	1688±5	U-Pb age—zircon	USGS/W. Premo
RGR–02	432719	4103875	4.21±0.13	$^{40}Ar/^{39}Ar$—whole rock, plateau age	USGS/M. Cosca
RGR–03	443405	4107035	1.06±0.04	$^{40}Ar/^{39}Ar$—whole rock, plateau age	USGS/M. Cosca
RGR–104	428382	4116917	26.97±0.14	$^{40}Ar/^{39}Ar$—whole rock, isochron age	USGS/M. Cosca
RGR–138	439704	4120766	24.52±0.13	$^{40}Ar/^{39}Ar$—whole rock, plateau age	USGS/M. Cosca
RGR–474	427077	4099928	25.36±0.09	$^{40}Ar/^{39}Ar$—whole rock, integrated age	USGS/M. Cosca
RGR–490	427058	4100633	25.22±0.05	$^{40}Ar/^{39}Ar$—whole rock, integrated age	USGS/M. Cosca
SA–MM06–90	455323	4113291	4.74±0.19	$^{40}Ar/^{39}Ar$—groundmass concentrate, plateau age	USGS/D. Miggins
SLH501	435081	4112675	5.19±0.11	$^{40}Ar/^{39}Ar$—groundmass concentrate, plateau age	USGS/D. Miggins
SLH502	435240	4114819	29.6±0.2	$^{40}Ar/^{39}Ar$—biotite, plateau age	USGS/M. Cosca
SLH503	438414	4119137	28.88±0.05	$^{40}Ar/^{39}Ar$—biotite, plateau age	USGS/D. Miggins
SLH504	432392	4117495	27.67±0.04	$^{40}Ar/^{39}Ar$—sanidine, plateau age	USGS/D. Miggins
SLH504	432392	4117495	27.2±0.2	$^{40}Ar/^{39}Ar$—biotite, plateau age	USGS/M. Cosca
SLH504	432392	4117495	28.5±0.4	$^{40}Ar/^{39}Ar$—hornblende, plateau age	USGS/M. Cosca
SLH506	435825	4117529	28.82±0.09	$^{40}Ar/^{39}Ar$—biotite, plateau age	USGS/D. Miggins
SLH506	435825	4117529	28.7±0.3	$^{40}Ar/^{39}Ar$—biotite, plateau age	USGS/M. Cosca
SLH507	435296	4115178	30.33±0.06	$^{40}Ar/^{39}Ar$—groundmass concentrate, plateau age	USGS/D. Miggins
SLH508	428607	4104700	29.91±0.09	$^{40}Ar/^{39}Ar$—biotite, plateau age	USGS/D. Miggins
SLH508	428607	4104700	30.2±0.3	$^{40}Ar/^{39}Ar$—biotite, plateau age	USGS/M. Cosca
SLH509	428130	4101650	26.12±0.58	$^{40}Ar/^{39}Ar$—groundmass concentrate, plateau age	USGS/D. Miggins
SLH510	469308	4102812	29.01±0.12	$^{40}Ar/^{39}Ar$—biotite, plateau age	USGS/D. Miggins
SLH510	469308	4102811	29.3±0.3	$^{40}Ar/^{39}Ar$—biotite, plateau age	USGS/M. Cosca
SLH512	428515	4116219	27.93±0.09	$^{40}Ar/^{39}Ar$—sanidine, plateau age	USGS/D. Miggins
SLH512	428515	4116219	28.8±0.2	$^{40}Ar/^{39}Ar$—biotite, plateau age	USGS/M. Cosca
SLH512	428515	4116219	28.9±0.3	$^{40}Ar/^{39}Ar$—hornblende, plateau age	USGS/M. Cosca
SLH513	428429	4116712	26.79±0.21	$^{40}Ar/^{39}Ar$—groundmass concentrate, plateau age	USGS/D. Miggins
SLH514	422090	4114708	30.45±0.09	$^{40}Ar/^{39}Ar$—groundmass concentrate, plateau age	USGS/D. Miggins
SR1	460713	4102386	13.4±0.08	$^{40}Ar/^{39}Ar$—hornblende, plateau age	USGS/D. Miggins
SR12	455904	4096802	3.79±0.05	$^{40}Ar/^{39}Ar$—groundmass concentrate, plateau age	USGS/D. Miggins
SR7	460073	4100532	10.61±0.11	$^{40}Ar/^{39}Ar$—groundmass concentrate, plateau age	USGS/D. Miggins
T84089	427172	4099225	25.95±0.58	$^{40}Ar/^{39}Ar$—groundmass concentrate, plateau age	USGS/D. Miggins
T84150	427456	4117928	26.53±0.59	$^{40}Ar/^{39}Ar$—groundmass concentrate, plateau age	USGS/D. Miggins
T84163	426950	4110752	25.49±0.41	$^{40}Ar/^{39}Ar$—groundmass concentrate, plateau age	USGS/D. Miggins
TR–MM06–79	466697	4116823	4.69±0.30	$^{40}Ar/^{39}Ar$—groundmass concentrate, plateau age	USGS/D. Miggins

[1]U.S. Geological Survey (USGS), M. Cosca, Michael A. Cosca; D. Miggins, Daniel P. Miggins

Figure 4. Photograph of the Costilla Crossing Bridge over the Rio Grande. The bridge is a single lane, two-span Thatcher through-truss bridge constructed in 1892. It was posted to the National Register of Historic Places in 1985. The bridge is 11.5 km south of Colorado Hwy 142 bridge over the Rio Grande and accommodates local traffic in the southern San Luis Valley. Oligocene intrusive rocks (Tiq) of South Piñon Hills (left) and mesa-capping basaltic lava flows (Th) overlying andesite lava flows (Tcl) of Piñon Hills (right) are visible in background. The bridge rests on a single Servilleta Basalt (Tsb) lava flow likely erupted from vent(s) to the south. The bridge was restored in 2006. Photo by Ren A. Thompson, 2005.

Figure 5. Photograph of vertical vesicle pipes in an olivine tholeiite lava flow, characteristic of Servilleta Basalt (Tsb) in the southern part of the map area, San Pedro Mesa, and scattered outcrops along the western range front of the Sangre de Cristo Mountains. Photo by Ren A. Thompson, 2005.

Tbb **Basaltic andesite of San Pedro Mesa (Miocene)—**Dark-gray, fine-grained, basaltic andesite lava flows, associated breccia, and near-vent reddish-brown pyroclastic deposits. Contains small olivine phenocrysts that are typically partly altered to iddingsite, and locally minor xenocrysts of quartz and feldspar. Typically caps hills that rise above the surrounding plains of Servilleta Basalt (Tsb) of San Pedro Mesa and fills paleovalleys cut into the underlying andesite and dacite (Tba). Interbedded with sediments of the lower part of Santa Fe Group (Tsf). $^{40}Ar/^{39}Ar$ analysis of groundmass concentrate yielded an apparent age of 10.61±0.11 Ma (sample SR7; table 2). Thickness 110 m, base not exposed

Tb **Basaltic andesite and trachyandesite, undivided (Miocene)—**Light- to dark-gray porphyritic basalt and trachyandesite flows, flow breccias, and agglutinate. Basaltic rocks contain phenocrysts of olivine (typically altered to iddingsite), pyroxene and plagioclase; more evolved trachyandesite compositions contain pyroxene and plagioclase phenocrysts and subordinate amounts of hornblende and Fe-Ti oxides. Locally interbedded with sediments of the Santa Fe Group (Tsf). $^{40}Ar/^{39}Ar$ analysis of groundmass and mineral concentrates from a lava flow yielded apparent ages ranging from about 15 to 11 Ma (Miggins, 2002; Miggins and others, 2002; Kirkham and others, 2004). Thickness approximately 300 m

Tba **Andesite and dacite of San Pedro Mesa (Miocene)—**Light-gray to light-brown porphyritic andesite to dacite lava flows and flow breccias preserved in the south-central part of San Pedro Mesa. Phenocrysts of pyroxene, hornblende, and plagioclase are common, with lesser amounts of biotite, Fe-Ti oxides, and minor quartz. Phenocrysts vary considerably in size and proportion within map unit. $^{40}Ar/^{39}Ar$ analysis of groundmass concentrates from a lava flow yielded an apparent age of 13.4±0.08 Ma (sample SR1; table 2). This unit may be broadly correlative with unit Tb in the Culebra Range to the east. Thickness 50 m

Th **Hinsdale Formation (Oligocene)—**Basaltic lava, associated breccia, and near-vent pyroclastic deposits. Includes fine-grained silicic alkali-olivine basalt, basaltic andesite, tholeiitic basalt and minor andesite and xenocrystic basaltic andesite. Sparse small olivine phenocrysts partly altered to iddingsite are typical, and xenocrysts of quartz and feldspar are locally abundant. Typically forms flat-topped hills and mesas that are buried channels cut into unit Tcl in the San Luis Hills. K-Ar whole rock ages range from 26.4 to 25.7 Ma (Thompson and others, 1991). $^{40}Ar/^{39}Ar$ age determinations from lava flows at the base of the section at Flat Top yielded apparent ages of 26.79±0.21 Ma and 26.53±0.59 Ma (samples SLH513 and T84150; table 2). A lava flow capping Piñon Hills yielded an $^{40}Ar/^{39}Ar$ apparent age of 25.49±0.41 Ma (sample T84163; table 2) and lava flows from South Piñon Hills yielded $^{40}Ar/^{39}Ar$ apparent ages of 25.22±0.05 Ma and 25.95±0.58 Ma (samples RGR–490 and T84089; table 2) at the base of the section and 25.36±0.09 Ma near the top (sample RGR–474, table 2) and 26.12±0.58 Ma (sample SLH509; table 2) at an intermediate stratigraphic position. East of the Rio Grande, a basal lava flow of Music Mesa yielded an $^{40}Ar/^{39}Ar$ apparent ages of 24.52±0.13 Ma (sample RGR–138; table 2). Thickness 375 m

Conejos Formation (Oligocene)—Includes mafic to intermediate-composition vent facies rocks, lava flows, flow breccias, explosion breccias, and volcaniclastic rocks, principally mudflow breccias. Divided into an upper sequence (Tcu) and a lower sequence (Tcl) on the basis of observed stratigraphy and variations in flow morphology, mineralogy, and whole-rock geochemistry. Map unit restricted to the San Luis Hills in west-central part of mapped area

Tcu **Upper part—**Predominantly porphyritic andesite flows, breccias and mudflows, locally overlain by discontinuous exposures of sparsely porphyritic dacite lava flows. Andesites contain moderate abundances of pyroxene and plagioclase phenocrysts and lesser amounts of Fe-Ti oxides in a microcrystalline groundmass. Dacites contain sparse phenocrysts of plagioclase and hornblende and minor biotite and accessory Fe-Ti oxides. Thickness approximately 175 m

Tcl **Lower part—**Predominantly dark- to light-brown, sparsely porphyritic andesite flows and volcaniclastic breccias in lower part of section, locally overlain by massive, gray, glassy, coarsely porphyritic dacite lava flows, dome remnants, and mudflows. Andesites contain sparse to moderate amounts of pyroxene and plagioclase phenocrysts, and minor olivine and Fe-Ti oxides in a microcrystalline groundmass. Dacites contain moderate amounts

Figure 6. Photograph of view northwest from Costilla Crossing Bridge toward Piñon Hills. Flat Top mesas are capped by Oligocene basaltic lava flows of the Hinsdale Formation (Th) that are dominantly underlain by Oligocene andesite and dacite volcanic deposits of the lower Conejos Formation (Tcl). Photo by Ren A. Thompson, 2005.

of plagioclase, hornblende, biotite phenocrysts and minor pyroxene and Fe-Ti oxides. An andesite lava flow from the western margin of the San Luis Hills, near the confluence of the Rio San Antonio and Conejos River yielded an $^{40}Ar/^{39}Ar$ apparent age of 30.45±0.09 Ma (sample SLH514; table 2). South of the Hwy 142 bridge crossing, andesite and dacite lava flows exposed along the Rio Grande yielded $^{40}Ar/^{39}Ar$ apparent ages of 29.6±0.2 Ma and 30.33±0.06 Ma respectively (samples SLH502 and SLH507; table 2). Locally, dacite dikes intruding lava flows yielded $^{40}Ar/^{39}Ar$ apparent ages of 28.7±0.3 Ma (sample SLH506; table 2) in the Brownie Hills, and 28.9±0.3 Ma (sample SLH512; table 2) low on the southern flank of Flat Top. Thickness 450 m, base not exposed

Tv **Volcanic rocks, undivided (Oligocene)**—Andesite and dacite flows and flow breccias, weakly welded tuff and subordinate amounts of laharic breccia, and other volcaniclastic deposits exposed in Culebra Range and western Sangre de Cristo Mountains. Includes regionally identifiable light to dark brown, lithic-rich ash flow tuff near the base of this volcanic sequence that is characterized by phenocrysts of biotite, hornblende, plagioclase, minor sanidine, and locally quartz. $^{40}Ar/^{39}Ar$ analysis of sanidine concentrates yielded an apparent age of 29.6±0.1 Ma, (Wallace, 1996) and is at least temporally related, if not correlative with, early outflow facies from the Platoro caldera to the west in the San Juan Mountains. Lava flows are typically thin and discontinuous, but can be locally massive in dacite flows. Laharic breccias are brown with cobble- to boulder-size, angular to subrounded clasts and variable amounts of interstitial matrix. Volcaniclastic rocks are light brown to gray and are interbedded with massive to thinly laminated, poorly to well-sorted sediments. Thickness approximately 225 m

Tvl **Volcanic lahar and breccia deposits (Oligocene)**—Predominantly monolithologic andesite breccias, associated lava flows, and discontinuous volcaniclastic rocks exposed in the Culebra Range. Breccia is brown with angular to subrounded boulder-size clasts and variable amounts of interstitial matrix. Volcaniclastic rocks are light brown to gray interbedded with massive to thinly laminated, poorly to well-sorted sediment; laterally continuous volcaniclastic unit near middle of volcanic section contains abundant pumice and lithic clasts and forms massive, subrounded to thinly bedded outcrops. May be about 30 Ma, and, in part, age equivalent to the Conejos Formation (Tcu and (or) Tcl) in the San Luis Hills. Thickness approximately 150 m

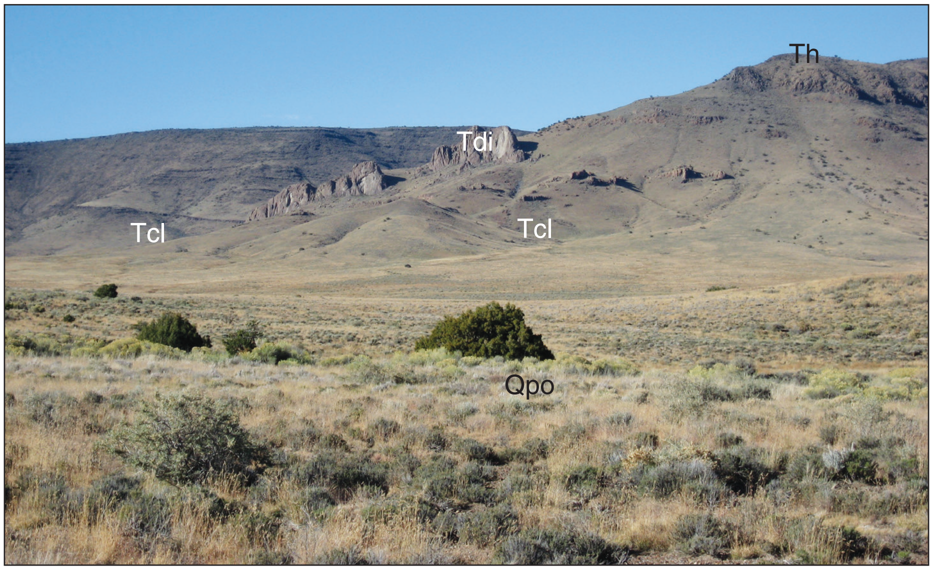

Figure 7. Photograph of view northwest toward the southern flanks of Flat Top in the San Luis Hills. Prominent fins of exposed bedrock in near hills are eroded remnants of vertical dacite dikes (Tdi) cutting andesite lava flows and breccia deposits of the lower Conejos Formation (Tcl). Thinly bedded lava flows in far hills are basaltic and basaltic andesite lava flows of the Hinsdale formation (Th) erupted unconformably onto the deeply incised Conejos Formation deposits. Note the northeastern "fanning" dips of the Hinsdale Formation lava flows becoming progressively less tilted upsection, likely related to contemporaneous deposition of lava flows and interbedded deposits in the hanging wall of an active Oligocene down-to-west extensional fault (up valley and out of view in photo). Deposits of undivided alluvium and colluvium are visible in the foreground (Qpo). Photo by Ren A. Thompson, 2006.

INTRUSIVE ROCKS

Tdt **Dacite porphyry and tuff (Miocene)**—Intrusive phase is a light gray dacite porphyry with phenocrysts of plagioclase, potassium feldspar, quartz, hornblende, and biotite in a fine-grained holocrystalline groundmass. Mapped in an isolated large porphyry stock and a related smaller satellitic intrusion in southeast part of map area. Minimum $^{40}Ar/^{39}Ar$ age is 15.23 Ma (Kirkham and others, 2005). Locally includes volumetrically minor andesite dikes containing pyroxene and plagioclase phenocrysts in a microcrystalline groundmass and a medium gray (devitrified) to black (vitrophyric) welded ash-flow tuff dike and an extrusive welded ash-flow tuff, about 1 km south and 6 km southeast of large stock, respectively. These tuffs are petrographically indistinguishable having phenocrysts of plagioclase and acicular hornblende in a microcrystalline to glassy groundmass. Tuffs not shown at map scale

Ti **Intrusive rocks, undivided (Miocene and Oligocene)**—Lamprophyre, alkali basalt, and much lesser intermediate and silicic dikes, primarily associated with the Spanish Peaks intrusive complex (Ti). $^{40}Ar/^{39}Ar$ determinations from mineral separate concentrates yielded apparent ages ranging from 25 to 22 Ma (Penn and Lindsey, 1996; Miggins, 2002). Shown as both irregular intrusive bodies and linear dikes in the map area

Tgr **Rhyolite porphyry and dacite (Miocene and Oligocene)**—Stocks comprise porphyritic rhyolite and lesser dacite emplaced mainly along backthrusts that cut Pierre Shale and related formations (Kpu) in the eastern part of the map area. Probably related to and coeval with 25–22 Ma dikes of Spanish Peaks intrusive complex (Ti) (Miggins, 2002)

Tdi **Dacite porphyry (Oligocene)**—Predominantly northeast-trending dikes and small stocks of coarsely porphyritic dacite. Phenocrysts consist of plagioclase, sanidine, biotite, hornblende, Fe-Ti oxides, and minor quartz; xenocrysts are resorbed oligoclase. Confined to the San Luis Hills area; commonly intrudes Conejos Formation rocks. Locally includes dikes of sparsely porphyritic to porphyritic andesite containing plagioclase, clinopyroxene, and plagioclase. Sanidine concentrates from a small dacite intrusion in the Fairy Hills (too small to show at map scale) yielded $^{40}Ar/^{39}Ar$ apparent sanidine and biotite ages of 27.67±0.04 and 27.2±0.2 Ma respectively (sample SLH504, table 2)

Tiq **Quartz monzonite (Oligocene)—**Gray to light tan, fine- to medium-grained quartz monzonite; equigranular to slightly porphyritic; contains potassium feldspar, plagioclase, quartz, variably altered biotite, iron-titanium oxides, and minor clinopyroxene. Locally includes one small stock that comprises gray, equigranular, medium-grained diorite containing plagioclase, clinopyroxene, olivine, and iron-titanium oxides. Aplite dikes commonly intrude the stocks. Present in several areas as steep-sided stocks along north-trending belt in the San Luis Hills (Thompson and Machette, 1989). $^{40}Ar/^{39}Ar$ age determinations on biotite yield an apparent age of 29.3±0.3 Ma (sample SLH510; table 2)

PALEOGENE SEDIMENTARY ROCKS

Tcs **Conglomerate and sandstone (Oligocene?)—**Dark maroon to red, poorly sorted, strongly iron-stained conglomerate and sandstone that are locally exposed in the western Sangre de Cristo Mountains. Unit previously mapped by Wallace and Lindsey (1996), and Wallace and Soulliere (1996) as the Vallejo Formation of Upson (1941). Rounded clasts in the conglomerate were derived chiefly from Paleozoic and Proterozoic rocks, although some deposits are composed almost entirely of Proterozoic gneiss and quartzite clasts. Subangular boulders, as large as 2 m in diameter, are locally exposed near the base. Unit may correlate with a boulder conglomerate (clasts 1–3 m diameter) exposed beneath volcanic rocks along the western margin of San Pedro Mesa (unit Tvl of Thompson, Machette, and Drenth, 2007) where the boulder conglomerate contains volcanic clasts dominated by lithic-rich, moderately welded ash-flow tuff. Tuff clasts are likely derived from Treasure Mountain Group deposits (29.5–28.5 Ma) associated with recurrent subsidence at the Platoro caldera complex in the southeastern San Juan Mountains (Lipman, 1975, 2006; Dungan and others, 1989). Thickness approximately 100 m

Tch **Cuchara Formation (Eocene)—**Interbedded conglomerate, sandstone, and mudstone (upper member) about 800 m thick, underlain by interbedded arkosic sandstone, mudstone, and conglomerate (lower member) about 300–550 m thick. Rounded clasts derived from Paleozoic and Proterozoic rocks of Sangre de Cristo Mountains. Present only in northeast corner of map. Composite thickness 1,100–1,350 m

PALEOCENE AND OLDER SEDIMENTARY ROCKS

TKs **Poison Canyon and Raton Formations, undivided (Paleocene and Upper Cretaceous)—**Deltaic coarsening-upward sequence consisting of yellowish-tan sandstone, sandstone-matrix conglomerate, siltstone, and black shale, with coal beds in the Raton Formation (mainly in lower part). Temporally equivalent and interfingers locally. Maximum thicknesses about 60 m (Poison Canyon Formation) and about 250 m (Raton Formation)

Kvt **Vermejo Formation and Trinidad Sandstone, undivided (Upper Cretaceous)—**Vermejo Formation consists of shale, siltstone, coal, and lesser sandstone deposited in a distal deltaic-lagoon environment. Trinidad Sandstone consists of light-tan sandstone deposited in a beach-barrier-bar environment; units are undivided at the map scale. Maximum composite thickness about 30 m

Kpu **Pierre Shale, Niobrara Formation, Carlile Shale, Greenhorn Limestone, and Graneros Shale, undivided (Upper Cretaceous)—**Black marine shale with minor interbeds of poorly sorted sandstone and limestone. Locally, shale units are mantled by colluvium (Qc), are deformed by creep and other mass-movement processes, and include unmapped landslide deposits. Thicknesses from top down are about 550 m of Pierre Shale, about 200 m of Niobrara Formation, about 80 m of Carlile Shale, about 35 m of Greenhorn Limestone, and about 35 m of Graneros Shale

Kdp **Dakota Sandstone and Purgatoire Formation, undivided (Lower Cretaceous)—**Dakota Sandstone consists of fine-grained, well-sorted and well-cemented, mainly massive tan sandstone and rare conglomerate, about 20 m thick. Underlying Purgatoire Formation consists of about 70 m of fissile dark-brown shale and medium-gray limestone containing cylindrical nodules of red chert

Js **Jurassic sedimentary rocks, undivided—**Includes bentonitic siltstone of Morrison Formation and eolian-derived Entrada Sandstone; both are off-white and about 20 m thick

JꞮs **Jurassic and Triassic sedimentary rocks, undivided—**See descriptions of Jurassic sedimentary rocks, undivided (Js) and Triassic sedimentary rocks, undivided (TRs). Thickness approximately 200 m

Ꞁs **Triassic sedimentary rocks, undivided—**Includes arkosic sandstone, siltstone, and shale with minor bentonitic beds; thickness and lower boundary uncertain

PꞒs **Sangre de Cristo Formation (Lower Permian to Middle Pennsylvanian)—**Thick sequence of mainly terrestrial rocks consisting of red arkosic sandstone, conglomeratic sandstone, siltstone, shale, and local gray limestone arranged in fining-upward alluvial cycles about 1–10 m thick. Sandstone and conglomeratic sandstone is cross-bedded; siltstone and shale contain ripple marks, cross-laminations, and mud cracks. Marker bed composed of thin, fossiliferous, marine limestone is about 30–60 m above the base of the formation (Lindsey, 1995a,b; Wallace and Lindsey, 1996; Fridrich and Kirkham, 2007). Maximum thickness >4,000 m

Ꞓm **Madera Formation (Middle Pennsylvanian) and Sandia Formation (Middle and Lower Pennsylvanian), undivided—**Thick sequence of marine and non-marine rocks consisting of multiple stratigraphic sequences composed of terrestrial conglomerates, sandstones, and siltstones alternating with marine limestone and black shale. From top to bottom, includes Whiskey Creek Pass Limestone Member of Madera Formation of Brill (1952) and subjacent calcareous beds, arkose member (arkosic limestone member of Madera Formation of Brill, 1952), and gray limestone member of Madera Formation and Sandia Formation (Lindsey, 1995a,b; Wallace and Lindsey, 1996). Maximum thickness about 1,700 m

LOWER PALEOZOIC OR NEOPROTEROZOIC INTRUSIVE IGNEOUS ROCKS

PzZg **Gabbro dikes and intrusive bodies (early Paleozoic? or Neoproterozoic?)—**Dikes and larger intrusive bodies composed of non-foliated pyroxene gabbro that cut foliated Paleoproterozoic rocks but not Middle Pennsylvanian sedimentary rocks, such as the Madera, Sandia, and Sangre de Cristo Formations. Dikes also shown as lines on map where extent or configuration of unit cannot be portrayed as a polygon

PALEOPROTEROZOIC METAIGNEOUS AND METASEDIMENTARY ROCKS

Xp **Pegmatite**—Granitic pegmatite and lesser aplite exposed as dikes, sills, and irregular masses, most of which are smaller than 1 km^2 in area. Only mapped along the western edge of the Sangre de Cristo Mountains, in the eastern part of the map area (Fridrich and Kirkham, 2007)

Xma **Amphibolite—**Amphibolite of generally basaltic composition in meta-extrusive layers, meta-intrusive dikes, and larger bodies; locally includes bodies of hornblendite. Commonly forms tabular bodies within unit Xms in the western part of the Culebra Range and central part of Sangre de Cristo Mountains

Xg **Gneissic monzogranite of State Line Peak area—**Weakly to strongly foliated monzogranite. Mapped in the southern part of the Culebra Range Sensitive High Resolution Ion Microprobe (SHRIMP) U-Pb zircon ages dating of rocks from this unit in the valleys of Jaroso Creek and Alamosito Creek yielded concordant ages of 1,688±5 Ma and 1,688±7 Ma, respectively (samples JI–1XGG1 and ACX–99; table 2)

Xag **Augen gneiss of Carneros Creek area—**Moderately to strongly foliated granodiorite or quartz monzonite. Commonly has a strong augen texture. Mapped in the northern part of the Culebra Range on the western and southwestern flank of Culebra Peak. SHRIMP U-Pb zircon dating of rock from this unit in the valley of Alamosito Creek yielded an age of 1,716±6 Ma (sample CF7–28–09–1; table 2)

Xgg **Granitic orthogneiss and monzogranite of Trinchera Peak area—**Lithologically variable unit across the map area. Mostly leucocratic augen gneiss, hornblende gneiss, and felsic gneiss in the central and northern Sangre de Cristo Mountains of the map area. In the Culebra Range deposit, are chiefly moderate to strongly foliated, leucocratic monzogranite. SHRIMP U-Pb zircon dating of igneous and metamorphic rocks collected south of Blanca Peak 10 km north of the map area yielded ages of 1,724±6 Ma for augen gneiss, 1,729±5 Ma for biotite tonalite, and 1,729±5 Ma for metagabbro(?) (W.R. Premo, USGS, written commun., 2013)

Xsv **Interbedded metasedimentary and metavolcanic rocks, undivided—**Unit consisting of interbedded metasedimentary rocks (mainly biotite-muscovite-quartz-feldspar schist) and metavolcanic rocks (Xmv). The latter consists mainly of bodies of amphibolite and granitic gneiss. Only mapped in two locations in the eastern half of the map area in the western Sangre de Cristo Mountains

Xmv **Metavolcanic rocks—**Gneisses consisting of numerous layers of differing igneous compositions including tonalite, diorite, granodiorite, granite, and lesser amphibolite that locally exhibits relict textures of their volcanic protolith. Mapped in the Culebra Range and throughout the western part of the Sangre de Cristo Mountains. SHRIMP U-Pb zircon dating of rocks in this unit in the valley of Alamosito Creek yielded ages of 1,714±18 Ma for felsic gneiss (metadacite?) and 1,716±6 Ma for tonalitic gneiss (samples CF7–28–09–3 and CF7–28–09–1; table 2)

Xms **Metasedimentary rocks—**Mainly interbedded quartzite and muscovite-quartz schist, but also includes stratigraphically lower facies of biotite-muscovite-quartz-feldspar schist, and upper facies of orthoquartzite. Locally includes amphibolite beds that are too small to show at map scale, mainly in lower facies. Mapped in the western part of the Culebra Range. SHRIMP U-Pb zircon dating of orthoquartzite from this unit yielded a maximum age of 1,691±5 Ma (sample EVC–CF05–8; table 2)

Xr **Alkali granite gneiss—**Well foliated and very massive and internally homogeneous. Mapped in the western part of the Culebra Range of the Sangre de Cristo Mountains. SHRIMP U-Pb zircon dating of rock from this unit in the valley of Alamosito Creek yielded an age of 1,703±5 Ma (sample CF7–28–09–4; table 2)

Acknowledgments

Daniel P. Miggins, U.S. Geological Survey, dated Neogene volcanic rocks using the $^{40}Ar/^{39}Ar$ method. Wayne R. Premo, U.S. Geological Survey, dated Proterozoic basement rocks using the U-Pb zircon (SHRIMP) method. Kenzie Turner and Mark Hudson of the U.S. Geological Survey assisted with fault interpretations in the San Luis Hills. The authors thank Paul Carrara and David Lidke of the U.S. Geological Survey for their thorough reviews that greatly improved the report.

References Cited

American Geological Institute, 1982, Grain-size scales used by American geologists, modified Wentworth scale, in data sheets (2d ed.): Falls Church, Va, American Geological Institute, sheet 17.1.

Appelt, R.M., 1998, $^{40}Ar/^{39}Ar$ geochronology and volcanic evolution of the Taos Plateau volcanic field, northern New Mexico and southern Colorado: Socorro, New Mex. Institute of Mining and Technology, M.S., thesis, 58 p.

Barsch, Dietrich, 1987, The problem of ice-cored rock glaciers, *in* Shroder, J.F., and Vitek, J.D., eds., Rock glaciers: London, Allen and Unwin, p. 45–53.

Benedict, J.B., 1973, Chronology of cirque glaciation, Colorado Front Range: Quaternary Research, v. 3, p. 585–599.

Benson, Larry, Madole, Richard, Kubik, Peter, and McDonald, Richard, 2007, Surface-exposure ages of Front Range moraines that may have formed during the Younger Dryas, 8.2 cal ka, and Little Ice Age events: Quaternary Science Reviews, v. 26, p. 1638–1649.

Benson, L.V., Madole, R.F., Landis, G.P., and Gosse, John, 2005, New data for late Pleistocene alpine glaciation from southwestern Colorado: Quaternary Science Reviews, v. 24, p. 46–65.

Benson, L.V., Madole, R.F., Phillips, William, Landis, G.P., Thomas, Terry, and Kubic, P.W., 2004, The probable importance of snow and sediment shielding on cosmogenic ages of north-central Colorado Pinedale and pre-Pinedale moraines: Quaternary Science Reviews, v. 23, p. 193–206.

Birkeland, P.W., 1999, Soils and geomorphology: New York, Oxford University Press, 430 p.

Brill, K.G., Jr., 1952, Stratigraphy in the Permo-Pennsylvanian zeugogeosyncline of Colorado and northern New Mexico: Geological Society of America Bulletin, v. 63, p. 809–880.

Burroughs, R.L., 1972, Geology of the San Luis Hills, south-central Colorado: Albuquerque, University of New Mexico, Ph.D. dissertation, 139 p.

Cosca, M.A., Thompson, R.A., and Turner, K.J., 2014, High precision $^{40}Ar/^{39}Ar$ geochronology of Servilleta basalts of the Rio Grande gorge, New Mexico [abs.], *in* 2014 Fall Meeting, San Francisco, Calif., December 15–19, 2014: San Francisco, Calif., American Geophysical Union, Abstract V51A–4728.

Dahms, D.E., 2004, Relative and numeric age data for Pleistocene glacial deposits and diamictons in and near Sinks Canyon, Wind River Range, Wyoming: Arctic, Antarctic, and Alpine Research, v. 36, p. 59–77.

DigitalGlobe, Inc., 2012, GeoEye: Longmont, Colo., DigitalGlobe [Available at https://www.digitalglobe.com/resources/satellite-information.]

Drenth, B.J., Turner, K.J., Thompson, R.A., Grauch, V.J.S., Cosca, M.A., and Lee, J.P., 2011, Geophysical expression of elements of the Rio Grande rift in the northeast Tusas Mountains-Preliminary Interpretations, *in* Koning, D.J., Karlstrom, K.E., Kelley, S.A., Lueth, V.W., and Abby, S.B., eds., Geology of the Tusas Mountains and Ojo Caliente Area: New Mexico Geological Society 62d Annual Fall Field Conference, p. 165–175. [Available at http://nmgs.nmt.edu/publications/guidebooks/62/.]

Drenth, B.J., Grauch, V.J.S., and Rodriguez, B.D., 2013, Geophysical constraints on Rio Grande rift structure in the central San Luis Basin, Colorado and New Mexico, *in* Hudson, M.R., and Grauch, V.J.S., eds., New Perspectives on Rio Grande Rift Basins—From tectonics to groundwater: Boulder, Colo., Geological Society of America, Special Paper 494, p. 75–99, doi:10.1130/2013.2494(04).

Dungan, M.A., Lipman, P.W., Colucci, M.T., Ferguson, K.M., and Balsley, S.D., 1989, Southeastern (Platoro) caldera complex, *in* Lipman, P.W., ed., IAVCEI fieldtrip guide—Oligocene-Miocene San Juan volcanic field, Colorado: New Mexico Bureau of Mines and Mineral Resources Memoir 46, p. 305–329.

Fridrich, C.J., and Kirkham, R.M., 2007, Geologic map of the Culebra Peak area, Las Animas and Costilla Counties, Colorado: U.S. Geological Survey Open-File Report 2007–1428, scale 1:50,000. [Available at http://pubs.usgs.gov/of/2007/1428/.]

Huntley, David, 1979, Cenozoic faulting and sedimentation in northern San Luis Valley: Geological Society of America Bulletin, v. 90, p. 8–10.

Janke, J.R., 2007, Colorado Front Range rock glaciers—Distribution and topographic characteristics: Arctic, Antarctic, and Alpine Research, v. 39, p. 74–83.

Kirkham, R.M., and Heimsoth, C.M., 2002, Geologic map of the Fort Garland Southwest quadrangle, Costilla County, Colorado: Colorado Geological Survey Open-File Map 02–06, scale 1:24,000. [Available at http://store.coloradogeologicalsurvey.org/product/geologic-map-of-fort-garland-sw-quadrangle-costilla-county-colorado/.]

Kirkham, R.M., Keller, J.W., Price, J.B., and Lindsay, N.R., 2005, Geologic map of the southern half of the Culebra Peak quadrangle, Costilla and Las Animas County, Colorado: Colorado Geological Survey Open-File Map 05–03, scale 1:24,000. [Available at http://store.coloradogeologicalsurvey.org/product/geologic-map-of-the-southern-half-of-the-culebra-peak-quadrangle-costilla-and-las-animas-counties-colorado-2/.]

Kirkham, R.M., Lufkin, J.L., Lindsay, N.R., and Dickens, K.E., 2004, Geologic map of the La Valley quadrangle, Costilla County, Colorado: Colorado Geological Survey Open-File Map 04–08, scale 1:24,000. [Available at http://store.coloradogeologicalsurvey.org/product/geological-map-of-la-valley-7-5-minute-quadrangle-costilla-county-2/.]

Kirkham, R.M., Shaver, K.C., Lindsay, N.R., and Wallace, A.R., 2003, Geologic map of the Taylor Ranch quadrangle, Costilla County, Colorado: Colorado Geological Survey Open-File Map 03–15, scale 1:24,000. [Available at http://store.coloradogeologicalsurvey.org/product/geologic-map-of-the-taylor-ranch-quadrangle-costilla-county-colorado/.]

Lanphere, M.A., Champion, D.E., Christiansen, R.L., Izett, G.A., and Obradovich, J.D., 2002, Revised ages for tuffs of the Yellowstone Plateau volcanic field—Assignment of the Huckleberry Ridge Tuff to a new geomagnetic polarity event: Geological Society of America Bulletin, v. 114, p. 559–568.

Licciardi, J.M., and Pierce, K.L., 2008, Cosmogenic exposure-age chronologies of Pinedale and Bull Lake glaciations in greater Yellowstone and Teton Range, USA: Quaternary Science Reviews: v. 27, p. 814–831.

Lindsey, D.A., 1995a, Geologic map of the Cuchara quadrangle, Huerfano County, Colorado: U.S. Geological Survey, Miscellaneous Field Studies Map MF–2283, scale 1:24,000. [Available at http://ngmdb.usgs.gov/Prodesc/proddesc_5903.htm.]

Lindsey, D.A., 1995b, Geologic map of the McCarty Park quadrangle, Costilla and Huerfano Counties, Colorado: U.S. Geological Survey, Miscellaneous Field Studies Map MF–2282, scale 1:24,000. [Available at http://ngmdb.usgs.gov/Prodesc/proddesc_5902.htm.]

Lindsey, D.A., 1996, Reconnaissance geologic map of the Cuchara Pass quadrangle, Huerfano and Las Animas Counties, Colorado: U.S. Geological Survey, Miscellaneous Field Studies Map MF–2294, scale 1:24000. [Available at http://ngmdb.usgs.gov/Prodesc/proddesc_5914.htm.]

Lipman, P.W., 1975, Evolution of the Platoro caldera complex and related volcanic rocks, southeastern San Juan Mountains, Colorado: U.S. Geological Survey Professional Paper 852, 128 p. [Available at http://pubs.usgs.gov/pp/0852/report.pdf.]

Lipman, P.W., 2006, Geologic map of the central San Juan caldera cluster, southwestern Colorado: U.S. Geological Survey Geologic Investigation Series I–2799, scale 1:50,000. [Available at http://pubs.usgs.gov/imap/i2799/.]

Machette, M.N., 1985, Calcic soils of the southwestern United States, *in* Weide, D.L., ed., Soils and Quaternary geology of the southwestern United States: Geological Society of America Special Paper 203, p. 1–21.

Machette, M.N., and Puseman, K., 2007, Chapter E—Holocene sand deposits in the San Luis Basin, east of Alamosa Colorado, *in* Machette, M.N., Coates, M.M., and Johnson, M.J., eds., Quaternary geology of the San Luis Basin, southern Colorado and Northern New Mexico—Rocky Mountain Section Friends of the Pleistocene Guidebook, September 7–9, 2007: U.S. Geological Survey Open-File Report 2007–1193, p. 138–146.

Machette, M.N., Marchetti, D.W., and Thompson, R.A., 2007, Ancient Lake Alamosa and the Pliocene to middle Pleistocene evolution of the Rio Grande, chap. G, *of* Machette, M.N., Coates, M-M., and Johnson, M.L., eds., 2007 Rocky Mountain Section Friends of the Pleistocene field trip—Quaternary geology of the San Luis Basin of Colorado and New Mexico, September 7–9, 2007: U.S. Geological Survey Open-File Report 2007–1193, p. 157–168. [Available at http://pubs.usgs.gov/of/2007/1193/.]

Machette, M.N., and Thompson, R.A., 2005, Preliminary geologic map of the northwestern part of the Alamosa 30′ × 60′ quadrangle, Alamosa and Conejos Counties, Colorado: U.S. Geological Survey Open-File Report 2005–1392, scale 1:50,000. [Available at http://pubs.usgs.gov/of/2005/1392/.]

Machette, M.N., and Thompson, R.A., 2008, Preliminary geologic map of the north-central part of the Alamosa 30′ × 60′ quadrangle, Alamosa, Conejos, and Costilla Counties, Colorado: U.S. Geological Survey Open-File Report 2008–1124, scale 1:50,000. [Available at http://pubs.usgs.gov/of/2008/1124/.]

Machette, M.N., Thompson, R.A., and Drenth, B.J., 2008, Geologic map of the San Luis quadrangle, Costilla County, Colorado: U.S. Geological Survey Scientific Investigations Map 2963, scale 1:24,000. [Available at http://pubs.usgs.gov/sim/2963/.]

Machette, M.N., Thompson, R.A., Marchetti, D.W., and Smith, R.S.U., 2013, Evolution of ancient Lake Alamosa and integration of the Rio Grande during the Pliocene and Pleistocene, *in* Hudson, M.R., and Grauch, V.J.S., eds., New Perspectives on Rio Grande Rift basins—From tectonics to groundwater: Geological Society of America Special Paper 494, p. 1–20.

Madole, R.F., 1986, Lake Devlin and Pinedale glacial history, Front Range, Colorado: Quaternary Research, v. 25, p. 43–54.

Meierding, T.C., and Birkeland, P.W., 1980, Quaternary glaciation of Colorado, *in* Kent, H.C., and Porter, K.W., eds., Colorado geology: Rocky Mountain Association of Geologists Symposium Proceedings, Denver, Colorado, p. 165–173.

Miggins, D.P., 2002, Chronologic, geochemical, and isotopic framework of igneous rocks within the Raton basin and adjacent Rio Grande rift, south-central Colorado and northern New Mexico: Boulder, University of Colorado, M.S. thesis, 417 p.

Miggins, D.P., Thompson, R.A., Pillmore, C.L., Snee, L.W., and Stern, C.R., 2002, Extension and uplift of the northern Rio Grande rift—Evidence from $^{40}Ar/^{39}Ar$ geochronology from the Sangre de Cristo Mountains, south-central Colorado and northern New Mexico, *in* Menzies, M.A., Klemperer, S.L., Ebinger, C.J., and Baker, J., eds., Volcanic Rifted Margins: Geological Society of America Special Paper 362, p. 47–64.

Nelson, A.R., Millington, A.C., Andrews, J.T., and Nichols, H., 1979, Radiocarbon-dated upper Pleistocene glacial sequence, Fraser Valley, Colorado Front Range: Geology, v. 7, p. 410–414.

North American Commission on Stratigraphic Nomenclature, 1983, North American stratigraphic code: North American Commission on Stratigraphic Nomenclature. [Available at http://www.nacstrat.org/.]

Penn, B.S., and Lindsey, D.A., 1996, Tertiary igneous rocks and Laramide structure and stratigraphy of the Spanish Peaks region, south-central Colorado—Road log and descriptions from Walsenburg to La Veta (first day) and La Veta to Aguilar (second day), *in* Thompson, R.A., Hudson, M.R., and Pillmore, C.L., eds., Geologic Excursions to the Rocky Mountains and Beyond, Fieldtrip Guidebook for the 1996 Annual Meeting, Geological Society of America, Denver, Colorado, October 28–31: Geological Society of America Special Publication no. 44, (CD-ROM).

Pierce, K.L., 2004, Pleistocene glaciation of the Rocky Mountains, *in* Gillespie, A.R., Porter, S.C., and Atwater, B.F., eds., The Quaternary Period in the United States: Amsterdam, Elsevier, p. 63–76.

Pierce, K.L., Muhs, D.R., Fosberg, M.A., Mahan, S.A., Rosenbaum, J.G., Licciardi, J.M., and Pavich, M.J., 2011, A loess-paleosol record of climate and glacial history over the past two glacial-interglacial cycles (~150 ka), southern Jackson Hole, Wyoming: Quaternary Research, v. 76, p. 119–141.

Richmond, G.M., and Fullerton, D.S., 1986, Introduction to Quaternary glaciations in the United States of America, *in* Richmond, G.M., and Fullerton, D.S., eds., Quaternary glaciations in the United States of America: Quaternary Science Reviews, v. 5, p. 3–10.

Rogers, K.L., Larson E.E., Smith, G.A., Katzman, Daniel, Smith, G.R., Cerling, T.E., Wang, Yang, Baker, R.G., Lohmann, K.C., Repenning, C.A., Petterson, P.E., and Mackie, Gerald, 1992, Pliocene and Pleistocene geologic and climatic evolution in the San Luis Valley of south-central Colorado: Paleogeography, Paleoclimatology, Paleoecology: v. 94, p. 55–86, doi:10.1016/0031-0182(92)90113-J.

Rogers, K.L., Repenning, C.A., Forester, R.M., Larson E.E., Hall, S.A., Smith, G.A., Anderson E., and Browen, T.J., 1985, Middle Pleistocene (Late Irvingtonian—Nebraska) climatic changes in south-central Colorado: National Geographic Research: v. 1, p. 535–663.

Sarna-Wojcicki, A.M., Pringle, M.S., and Wijbrans, Jan, 2000, New $^{40}Ar/^{39}Ar$ age of the Bishop Tuff from multiple sites and sediment rate calibration for the Matuyama-Brunhes boundary: Journal of Geophysical Research, v. 105, p. 21431–21443.

Schildgen, T.F., and Dethier, D.P., 2000, Fire and ice—Using isotopic dating techniques to infer the geomorphic history of Middle Boulder Creek, Colorado: Geological Society of America Abstracts with Programs, v. 32, no. 7, p. A18.

Schumann, R.R., and Machette, M.N., 2007, Late Pleistocene to early Holocene paleoecology of the “Mr. Peat” wetland deposit, Alamosa County, Colorado, chap. F *of* Machette, M.N., Coates, M-M., and Johnson, M.L., eds., 2007 Rocky Mountain Section Friends of the Pleistocene field trip—Quaternary geology of the San Luis Basin of Colorado and New Mexico, September 7–9, 2007: U.S. Geological Survey Open-File Report 2007–1193, p. 147–156. [Available at http://pubs.usgs.gov/of/2007/1193/.]

Sharp, W.D., Ludwig, K.R., Chadwick, O.A., Amundson, Ronald, and Glaser, L.L., 2003, Dating fluvial terraces by $^{230}Th/U$ on pedogenic carbonate, Wind River basin, Wyoming: Quaternary Research, v. 59, p. 139–150.

Siebenthal, C.E., 1910, Geology and water resources of the San Luis Valley, Colorado: U.S. Geological Survey Water-Supply Paper 240, 120 p. [Available at http://pubs.er.usgs.gov/publication/wsp240.]

Soil Survey Staff, 1999, Soil taxonomy—A basic system of soil classification for making and interpreting soil surveys (2d ed.): U.S. Department of Agriculture Handbook 436, 869 p.

Sturchio, N.C., Pierce, K.L., Murrell, M.T., and Sorey, M.L., 1994, Uranium-series ages of travertines and timing of the last glaciation in the northern Yellowstone area, Wyoming-Montana: Quaternary Research, v. 41, p. 265–277.

Thompson, R.A., and Machette, M.N., 1989, Geologic map of the San Luis Hills area, Conejos and Costilla Counties, Colorado: U.S. Geological Survey, Miscellaneous Investigations Series Map I–1906, scale 1:50,000. [Available at http://pubs.usgs.gov/mis/I-1906/.]

Thompson, R.A., Johnson, C.M., and Mehnert, H.H., 1991, Oligocene basaltic volcanism of the northern Rio Grande rift; San Luis Hills, Colorado: Journal of Geophysical Research, v. 96, p. 13577–13592.

Thompson, R.A., Machette, M.N., and Drenth, B.J., 2007, Preliminary geologic map of the Sanchez Reservoir and eastern part of the Garcia quadrangles, Costilla County, Colorado: U.S. Geological Survey Open-File Report 2007–1074, scale 1:24,000. [Available at http://pubs.usgs.gov/of/2007/1074/.]

Thompson, R.A., Machette, M.N., Shroba, R.R., and, Ruleman, C.A., 2007, Geology of Mesita volcano, Colorado—Eruptive history and implications for basin sedimentation during the Quaternary, chap. H *of* Machette, M.N., Coates, M-M., and Johnson, M.L., eds., 2007 Rocky Mountain Section Friends of the Pleistocene field trip—Quaternary geology of the San Luis Basin of Colorado and New Mexico, September 7–9, 2007: U.S. Geological Survey Open-File Report 2007–1193, p. 169–180. [Available at http://pubs.usgs.gov/of/2007/1193/.]

Thompson, R.A., Turner, K.J., Cosca, M.A., Drenth, B., Hudson, M.R., and Lee, John, 2013, Temporal and spatial constraints on the evolution of a Rio Grande rift sub-basin, Guadalupe Mountain area, northern New Mexico [abs.], *in* 2014 Fall Meeting, San Francisco, Calif., December 15–19, 2014: San Francisco, Calif., American Geophysical Union, Abstract T21A-2527.

U.S. Geological Survey Geologic Names Committee, 2010, Divisions of geologic time—Major chronostratigraphic and geochronologic units: U.S. Geological Survey Fact Sheet 2010–3059, 2 p. [Available at http://pubs.usgs.gov/fs/2010/3059/.]

Upson, J.E., 1941, The Vallejo Formation—New early Tertiary red-beds in southern Colorado: Journal of Science, v. 239, no. 8, p. 577–589.

Wallace, A.R., 1996, Geologic map of the Trinchera Ranch quadrangle, Costilla County, Colorado: U.S. Geological Survey, Miscellaneous Field Studies Map MF–2312–C, scale 1:24,000. [Available at http://ngmdb.usgs.gov/Prodesc/proddesc_5931.htm.]

Wallace, A.R. and Lindsey, D.A., 1996, Geologic map of the Trinchera Peak quadrangle, Costilla, Huerfano, and Las Animas Counties, Colorado: U.S. Geological Survey, Miscellaneous Field Studies Map MF–2312–A, scale 1:24,000. [Available at http://ngmdb.usgs.gov/Prodesc/proddesc_5929.htm.]

Wallace, A.R., and Machette, M.N., 2008, Revised geologic map of the Fort Garland quadrangle, Costilla County, Colorado: U.S. Geological Survey, Scientific Investigations Map 2965, scale 1:24,000. [Available at http://pubs.usgs.gov/sim/2965/.]

Wallace, A.R. and Soulliere, S.J., 1996, Geologic map of the Ojito Peak quadrangle, Costilla County, Colorado: U.S. Geological Survey, Miscellaneous Field Studies Map MF–2312–B, scale 1:24,000. [Available at http://ngmdb.usgs.gov/Prodesc/proddesc_5930.htm.]

White, S.E., 1976, Rock glaciers and block fields, review and new data, 1961 to 1968: Quaternary Research, v. 6, p. 77–97.

Publishing support provided by:
Denver Publishing Service Center, Denver, Colorado

For more information concerning this publication, contact:

Center Director, USGS Geosciences and Environmental Change Science Center
Box 25046, Mail Stop 980
Denver, CO 80225
(303) 236-5344

Or visit the Geosciences and Environmental Change Science Center Web site at:
http://gec.cr.usgs.gov/

This publication is available online at:
http://dx.doi.org/10.3133/sim3342

USGS

Thompson and others—**Geologic Map of the Alamosa 30′ × 60′ Quadrangle, South-Central Colorado**—Scientific Investigations Map 3342

ISSN 2329-132X (online)
http://dx.doi.org/10.3133/sim3342